BRNO UNIVERSITY OF TECHNOLOGY

VYSOKÉ UČENÍ TECHNICKÉ V BRNĚ

FACULTY OF MECHANICAL ENGINEERING

FAKULTA STROJNÍHO INŽENÝRSTVÍ

INSTITUTE OF SOLID MECHANICS, MECHATRONICS AND BIOMECHANICS

ÚSTAV MECHANIKY TĚLES, MECHATRONIKY A BIOMECHANIKY

DESIGN AND PROTOTYPING OF ELECTRONICS FOR MANIPULATION PLATFORM

NÁVRH A REALIZACE ELEKTRONIKY PRO POLOHOVACÍ PLATFORMU

MASTER'S THESIS

DIPLOMOVÁ PRÁCE

AUTHOR

AUTOR PRÁCE

Bc. Adam Ondryáš

SUPERVISOR

VEDOUCÍ PRÁCE

doc. Ing. Zdeněk Hadaš, Ph.D.

BRNO 2022

BRNO UNIVERSITY OF TECHNOLOGY
FACULTY OF MECHANICAL ENGINEERING

Assignment Master's Thesis

Institut:	Institute of Solid Mechanics, Mechatronics and Biomechanics
Student:	**Bc. Adam Ondryáš**
Degree programm:	Mechatronics
Branch:	no specialisation
Supervisor:	**doc. Ing. Zdeněk Hadaš, Ph.D.**
Academic year:	2021/22

As provided for by the Act No. 111/98 Coll. on higher education institutions and the BUT Study and Examination Regulations, the director of the Institute hereby assigns the following topic of Master's Thesis:

Design and prototyping of electronics for manipulation platform

Brief Description:

One of the main components of manipulator is its electronic control unit (ECU). When designing an ECU, it is necessary to take into consideration all the features of the manipulator such as a type of power supply, driving mechanisms, and communication protocols. The ECU design must also meet the spatial and economic demands. Another criteria for the design is high efficiency and a cooling system if necessary.
This thesis deals with a systematic design of an ECU with compliance to the given parameters of a single–purpose application.

Master's Thesis goals:

– analysis of used technical solution for autonomous manipulators
– concept of electronic control unit
– design of electronic control unit
– prototyping and testing of individual funcitons

Recommended bibliography:

MĚŘIČKA, Jiří a Zdeněk ZOUBEK, 1973. Obecná teorie elektrického stroje. B.m.: SNTL.

RICHARDS KEITH L. Introduction to Stepper Motors and Their Drives. Design Engineer's Sourcebook. CRC Press, 2018.

WILSON, Peter. The Circuit Designer's Companion. Oxford: Elsevier Science & Technology, 2017.

AYOUB, Elie a Nabil KARAMI. Review on the charging techniques of a Li-Ion battery. In: 2015 Third International Conference on Technological Advances in Electrical, Electronics and Computer Engineering (TAEECE). IEEE, 2015, s. 50-55.

KÖHL, Susanne a Dirk JEGMINAT. How to Do Hardware-in-the-Loop Simulation Right. 2005.

Deadline for submission Master's Thesis is given by the Schedule of the Academic year 2021/22

In Brno,

L. S.

prof. Ing. Jindřich Petruška, CSc. Director of the Institute	doc. Ing. Jiří Hlinka, Ph.D. FME dean

Abstrakt

Tato diplomová práce je součástí projektu, na kterém pracují dva studenti. Cílem projektu je navrhnout a realizovat řídicí systém pro polohovací platformy. Tento řídicí systém umožňuje napájet polohovací platformy baterií a také je bezdrátově řídit z PC. Projekt se detailně zabývá koncepcí jednotlivých funkcionalit řidicího systému, návrhem a prototypováním hardwaru řídicí jednotky, návrhem firmwaru pro řidící jednotku a návrhem softwaru uživatelského prostředí.

Částmi projektu, kterými se zabývá tato práce, je koncepce jednotlivých funkcionalit a návrh hardwaru řidící jednotky.

Hardware řídicí jednotky byl v rámci práce navržen, vyroben a úspěšně otestován. Výstupem práce je tedy vyrobený prototyp řídicí jednotky, který lze v rámci projektu dále rozvíjet.

Summary

This thesis is a part of the project of two students. The project aims to design a manipulation platform control system. This control system allows the manipulation platform to be battery-powered and wirelessly controlled. The project consists of the control system concept design and the design of an electronic control unit hardware, firmware, and user control software.

The parts of the project that this thesis deals with are the concept design of individual functions and the hardware design of the electronic control unit.

The electronic control unit hardware was designed, manufactured, and successfully tested. The result of this work is therefore a fully functional prototype of the electronic control unit, which can be further developed as a part of the project.

Klíčová slova

polohovací platforma, DPS, řídicí jednotka, nabíječka baterií, bezdrátové řízení, krokový motor, Bluetooth

Keywords

manipulation platform, PCB, electronic control unit, battery charger, wireless control, stepper motor, Bluetooth

Bibliographic citation

ONDRYÁŠ, A. *Design and prototyping of electronics for manipulation platform.* Brno: Brno University of Technology, Faculty of Mechanical Engineering, 2022. 82 pages, Master's thesis supervisor: doc. Ing. Zdeněk Hadaš, PhD..

Rozšířený abstrakt

Úvod

Pro manipulaci se vzorky v různých vědeckých i industriálních odvětvích se často používají polo či plně automatizované manipulátory. Pro případ polohování vzorku v rovině jsou využívány polohovací platformy.

Motory těchto platforem jsou obvykle řízeny řídicí jednotkou. Řídicí jednotka společně s napájecím zdrojem standardně nejsou součastí platformy a musí tedy být připojeny externím kabelem. Tato separace polohovací platformy s motory od řídicí jednotky s napájením vede k omezenému použití platformy v aplikacích, jako je třeba systém počítačové tomografie. V tomto systému je vzorek polohován v rovině vůči zdroji rentgenového záření a následně je skenován. Během skenování dochází k rotaci vzorku a tedy i celé polohovací platformy, na které je vzorek položen. Externí kabel zde tedy nelze použít, protože by docházelo k jeho namotávání. K řešení tohoto problému je potřeba navrhnout nový bezdrátový řidící systém, který lze implementovat dovnitř polohovacích platforem.

Tato diplomová práce je součástí projektu, na kterém pracují dva studenti. Cílem projektu je navrhnout a realizovat řídicí systém pro polohovací platformy. Tento řídicí systém umožňuje napájet polohovací platformy baterií a také je bezdrátově řídit z PC. Projekt se detailně zabývá koncepcí jednotlivých funkcionalit řídicího systému, návrhem a prototypováním hardwaru řídicí jednotky, návrhem firmwaru pro řidící jednotku a návrhem softwaru uživatelského prostředí.

Vlastní práce

První část práce rozebírá technické řešení řídicích systémů, které jsou použity v industriálních polohovacích platformách. Popisuje základní terminologii a uvádí systémový diagram standardního řidícího systému polohovací platformy. Dále se věnuje standardně používánému řídicímu hardwaru a softwaru. Rešerše se také věnuje technologii baterií a uvádí problematiku bezdrátového řízení v realném čase. Malá část je také věnována bezdrátové technologii Bluetooth, která je následně použita v prototypu řídicí jednotky.

V druhé části jsou definovány funkcionality řidícího systému, ze kterých je následně vytvořen koncepční diagram pro řidící jednotku. Hlavní funkcionality, které musí řídicí jednotka obstarávat jsou následující: polohovací jednotky pro osu X a Y, bezdrátová komunikace a modul spravující napájení řídicí desky. Taktéž je požadováno, aby byly rozměry řídicí jednotky co nejmenší, tak aby mohla být využita i ve velmi malých polohovacích platformách.

Třetí část se zabývá systematickým návrhem řídicí jednotky dle koncepčního diagramu. První hlavní část této kapitoly se zabývá implementací elektrických obvodů polohovacích jednotek pro osu X a Y. Zde jsou navrženy obvody budičů krokových motorů, které byly zvoleny pro tento prototyp Matušem Remišem v rámci jeho práce. Taktéž jsou zde přidány konektory pro enkodéry a následně jsou navrženy koncové snímače, které fungují na bázi detekce magnetického pole.

Druhá hlavní část této kapitoly se věnuje implementaci Bluetooth Low Energy modulu, který umožňuje bezdrátovou komunikaci s kontrolním PC softwarem.

Třetí hlavní část této kapitoly se zabývá návrhem obvodů modulu pro správu napájení řídící jednotky. Navržené obvody modulu spravují napájení jednotlivých komponentů řídicí jednotky, monitorování baterie, nabíjení baterie a bezpečné zapínání a vypínání řídicí jednotky pomocí tlačítka. Součástí tlačítka jsou indikační LED diody, které lze přepínat dle stavu zařízení. Součástí modulu je také funkcionalita vypínání a zapínání jednotlivých skupin obvodů, pomocí které lze snížit odběr proudu z baterie v době nepoužívání daných funkcionalit. Taktéž je zde přidána přepěťová, podpěťová, teplotní a nadproudová ochrana.

Kapitola se dále věnuje návrhu obvodů menších funkcionalit, které byly definovány v koncepčním diagramu řídicí jednotky. První z nich je externí nevolatilní paměť, jež je zde použita pro uložení dynamických parametrů platformy, které si uživatel může libovolně nastavovat. Další je pak obvod gyroskopu, jež je zde využit na sledování aktuálního natočení platformy vůči rentgenovému zdroji v systému počítačové tomografie. Tato informace usnadňuje operátorovi polohování vzorku. Jako poslední funkcionalita řídicí jednotky je zde implementován USB konektor, který slouží pro přímé připojení řídící jednotky k uživatelskému PC. Tuto funkci lze do budoucna použít pro upgrade firmwaru řídicí jednotky, či pro servisování systému.

Veškeré tyto funkcionality jsou následně řízeny jedním ARM Cortex M4 mikrokontrolérem, který byl pečlivě vybrán dle požadavků celého řídicího systému. Všechny komponenty řídicí jednotky jsou vybrány s důrazem na vysokou účinnost a to z důvodu prodloužení chodu platformy na jedno nabití baterie.

Práce se dále zabývá návrhem desky plošných spojů pro navržené obvody řídicí jednotky. Důraz je zde na důležitost rozložení komponentů, jelikož se jedná o desku s analogovými, digitálními i výkonovými obvody. Protože koncept vyžaduje minimalizaci rozměrů desky řídicí jednotky, je zvolena 6 vrstvá deska s oboustranným osazením. Výsledná deska řídicí jednotky, která obsahuje všechny výše zmíněné funkcionality, měří pouhých 56 mm x 81 mm.

Závěr

Navržená řídicí jednotka je vyrobena, osazena a jednotlivé navržené funkcionality jsou v rámci kapitoly 6 náležitě otestovány.

Výstupem práce je plně funknčí prototyp řídicí jednotky pro navržený řídicí systém manipulačních platforem. Tato řídicí jednotka je následně úspěšně použita během prototypování firmwaru a softwaru řídicího systému v rámci práce Matuše Remiše [31].

I declare that I have worked on this thesis independently under the supervision of doc. Ing. Zdeněk Hadaš, Ph.D., using the sources listed in the bibliography.

Adam Ondryáš

Brno . . . .

I would like to wholeheartedly thank my family and my partner Hannah, who were always supportive of my endeavors. I would also like to give my thanks to the supervisor doc. Ing. Zdeněk Hadaš, Ph.D. for valuable advice during the writing of the thesis, and to all the members of the Council of Hrnčířská for lending a helping hand during the years of study.

Adam Ondryáš

Contents

1 Introduction

The positioning of objects or samples is an important part of many processes in various industrial branches. The ever-growing performance and safety demands bring an increasing need to replace manual positioning processes with partly or fully automated manipulators. Based on the type of application, plenty of parameters, such as work area dimensions, load capacity, dynamical requirements, and positioning accuracy need to be taken into account.

Modern manipulators are complex systems with multiple degrees of freedom, and therefore they are able to position objects by using both translational and rotational motions. In applications where the planar positioning of an object is sufficient, complex manipulators can be replaced by more compact manipulation platforms.

Manipulation platforms are often used in the fields of scientific research and development. Applications that require precise repetitive positioning should utilize a platform with decent repeatability. Other applications are constrained by a small work area and require very high positioning accuracy. The field of microscopy is a typical example of the latter.

Another specific application of manipulation platforms is in the field of computer tomography (CT). By utilizing X-ray technology, these systems are able to create a 3D model of the internal structure of the object of interest. During the data acquisition process, the CT system rotates the object of interest around its vertical axis. To achieve good results, the object of interest must be properly positioned prior to the data acquisition process. The positioning takes time and requires an experienced operator.

CT systems are commonly used for quality control in multiple industries. In these applications, time-efficient solutions are very much sought-after, and therefore using an automated positioning solution such as the manipulation platform would be highly beneficial.

2 Motivation

The translational motion of motorized platforms is usually generated through linear, stepper, or servo motors. The motors of the platform are connected to the control system. The control system consists of a power supply, electronic control unit (ECU), and PC software. In standard applications, the ECU and the power supply reside outside of the manipulation platform due to their size and therefore need to be connected to the platform by an external cable. Because of the external cable connection, it is challenging to use these control systems in applications that require the whole manipulation platform to rotate together with the positioned sample (CT systems).

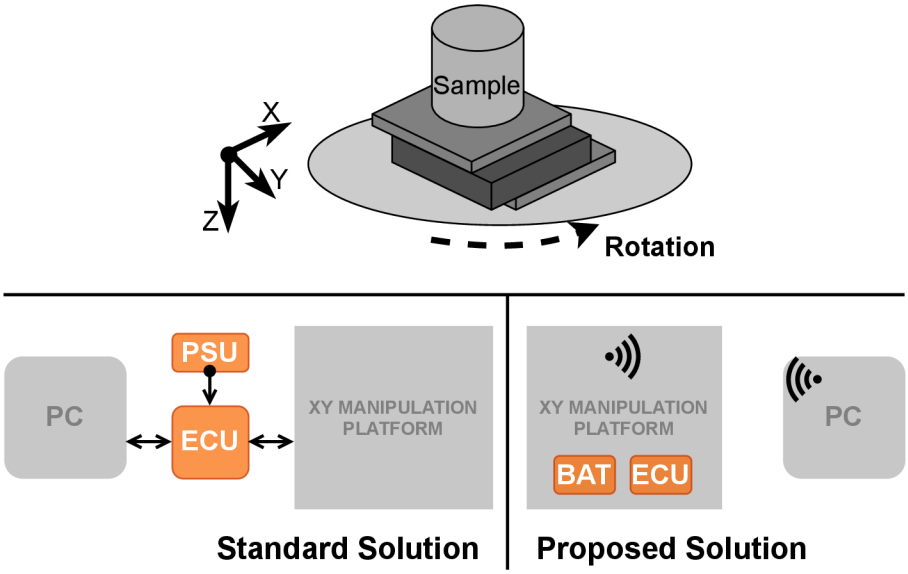

Figure 2.1: Standard Solution vs. Proposed Solution

2.1 Project Definition

With the drawback of the standard manipulation platform control systems in mind, the idea to develop a compact, plug-and-play manipulation platform control system, which is wireless and self-powered by a battery, has emerged. The proposed solution can be seen in the figure 2.1.

This project plans to design an electronic control unit hardware, firmware, and software, which can be implemented and used in various manipulation platform applications.

The controller hardware has to be very compact so that it can fit even inside very small manipulation platforms. It should be able to adapt to a range of power requirements and it must manage all the necessary functions of the manipulation platform. The firmware and software design have to be systematic and robust so that they can be thoroughly

tested and easily expanded upon when necessary. The software has to have a simple user interface for basic control and also a menu for more advanced functionalities.

2.2 Goals of the Project

- Conceptualize the functionalities of the platform control system
- Design and prototype an electronic control unit
- Design a firmware for the electronic control unit
- Design a software via which a user can control the manipulation platform
- Test the whole system on a prototype

2.2.1 Team Composition

Since the project requires knowledge from many different fields, it is assigned to two students. One student works on the electronics hardware, while the other works on the software and firmware. Planning and cooperation in certain areas of the project are crucial for the successful completion of the first functional prototype. The goals of the project (Figure 2.2) are divided between the two students in the following way:

Bc. Matuš Remiš

- Analyze positioning mechanisms of industrial manipulation platforms
- Design a motion unit for the prototype
- Design the electronic control unit firmware
- Design a software user interface for the manipulation platform control system

Bc. Adam Ondryáš (Author)

- Analyze technical solutions for autonomous manipulators
- Conceptualize the electronic control unit
- Design the electronic control unit
- Create a prototype and test individual functionalities of the electronic control unit

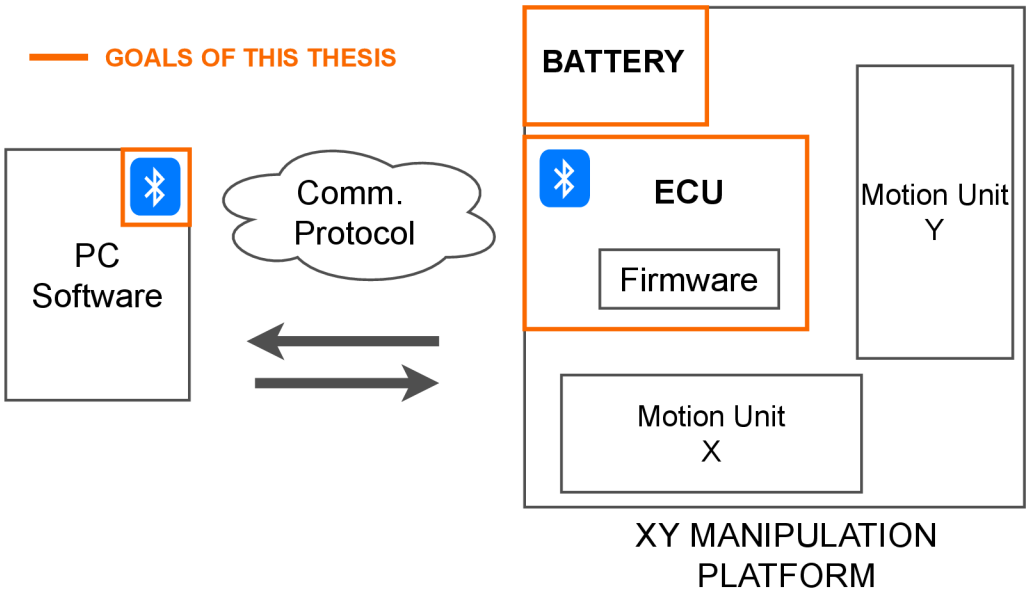

Figure 2.2: Goals of This Thesis with Respect to the Whole Project

3 Research

3.1 Manipulation Platforms

Nowadays, positioning platforms can vary from simple, manually operated machines, to complex, multi-axis motorized systems. Since this thesis deals with the design of the electronic control unit, only motorized systems are considered.

The manipulation platform is an electro-mechanical system and its performance and usability are defined by the synergic integration of used mechanical, electrical, firmware and software systems. The diagram in the Figure 3.1 shows the basic building blocks of the manipulation platform control system.

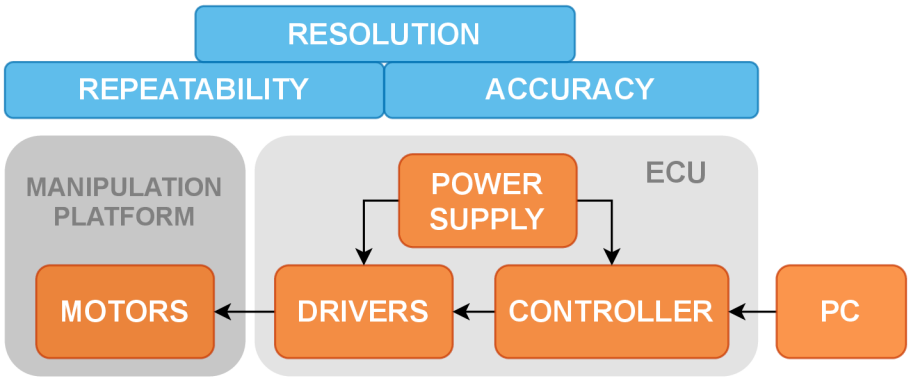

Figure 3.1: Diagram of a manipulation platform control system

3.1.1 Motion Basics Terminology

Each platform has a set of parameters that relate to its positioning qualities. An exhaustive list of such parameters exists. Most of the parameters are influenced by mechanical hardware design, manufacturing processes, assembly processes, etc. which are beyond the scope of this thesis. Therefore, only the most important and basic terms, where some of them can be influenced by the ECU design, are listed below. [1]

Resolution

Resolution is the smallest possible motion increment, that a system can be commanded to move. Sometimes it is referred to as display or encoder resolution. The fact that the system can be commanded to move by this amount does not mean it can do it consistently and precisely.

Minimum Incremental Motion

Minimum Incremental Motion is the smallest possible motion increment a system is capable of consistently delivering. This is sometimes referred to as Practical Resolution.

Accuracy

Accuracy is a measure of the degree, to which a given displacement complies with a standard. Environmental conditions, such as temperature, the test setup, and the procedure used to measure the displacement, can highly influence the accuracy of a manipulation platform. This applies mainly to the micron and submicron world, where thermal expansion can have a serious impact.

Repeatability

Repeatability is a measure of the manipulation platform's ability to repeatedly position to a specified point. Repeatability can be unidirectional or bidirectional, depending on how is the specified point approached. Systematic errors can be compensated, but the repeatability of the manipulation platform is the ultimate limit. The Figure 3.2 shows the relation between repeatability and accuracy. The middle of the target depicts the desired position value and each dot then corresponds with one positioning attempt.

Figure 3.2: Illustrative picture of accuracy vs. repeatability [2]

Vibrations

Vibrations are fast motions of small amplitude, which can be generated by airflow or electronics, such as a motor driver.

Velocity

Maximum velocity specification is generally provided at the manipulation platform's nominal load capacity. Higher velocities are possible with larger motor drivers, while minimum velocities are dependent on a manipulation platform's speed stability.

Speed Stability

Speed stability is a measure of the manipulation platform's ability to maintain constant velocity within defined limits. Usually, this is specified as a percentage of the desired velocity. Sometimes, this is referred to as Velocity Regulation. It is highly influenced by mechanical design, feedback mechanism, the motion controller, its control algorithm, and others.

3.1.2 Motor, Driver, Controller, and Software

There are many different types of motors that are used for varying tasks across the manipulation platforms industry [8].

Each type of motor needs a driver, which is a power circuit, specific to the used motor technology. The motor is then connected to the driver via a connector.

A controller is the logic unit, which implements the control algorithm, that tells the driver when and how to drive the motor[4] [6]. For more advanced systems, the controller also has inputs for various peripheral devices and sensors, such as encoders, limit switches, reference switches, etc. Another important feature of the controller is the communication interface, via which it can be connected to a PC.

Once connected, the PC software can be used to send commands to the controller, which then tells the driver how to move the motor so that the platform moves in the way the user desires [5]. The controller can have additional functionality such as a non-volatile memory, which can be utilized by the software to program the standalone operation of the manipulation platform, for example, a specific trajectory.

Drivers and controllers can be integrated into one unit and be powered by a single power supply. This is often done for low voltage devices. In this thesis, this kind of arrangement will be called the Electronic Control Unit (ECU). Last but not least, the ECU also usually features status indication LEDs and an ON/OFF power switch [7].

3.1.3 Industrial Example of Manipulation Platform

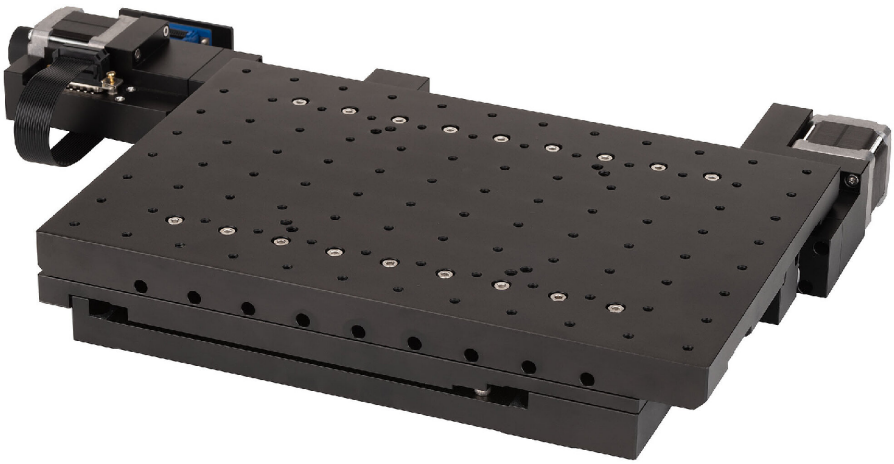

Figure 3.3: Industrial XY manipulation platform driven by two stepper motors [3]

A typical example of a manipulation platform can be seen in the Figure 3.3 , which is a model M-971 [9], produced by the company PI (Physik Instrumente). It is a price-sensitive XY manipulation platform. When it is paired with a proper ECU, it has decent positioning parameters, as can be seen in the Table 3.1. In the subsections below, a brief description of the used motor, driver, controller, and software technology is given.

Table 3.1: M-971 positioning specifications

Motion and positioning	Tolerance	Values
Active axes	-	X, Y
Resolution in X, Y	-	2.5 nm
Minimum incremental motion in X, Y	Typ.	0.2 μm
Unidirectional repeatablity in X, Y	Typ.	1 μm
Velocity in X, Y	Max.	10 mm/s

Stepper Motors

For applications with low velocity and decent precision requirements, stepper motors are the go-to technology. This manipulation platform uses stepper motors with the parameters in the Table 3.2 for both the X and Y-axis [9]. To produce the translational motion, it is using the most simple and inexpensive solution: a leadscrew with 1 mm pitch, which is connected to the motor shaft. Each axis also features a limit and a reference switch. It is meant to be driven in open-loop control since it does not feature an encoder.

Table 3.2: Properties of stepper motors used in M-971

Stepper motor parameters	Values
Nominal current RMS	1.2 A
Resistance	2.6 Ω
Inductance	1.9 mH
Motor resolution	400 $fullsteps/rev$

Driver and Controller

Figure 3.4: C-663.12 Mercury step controller

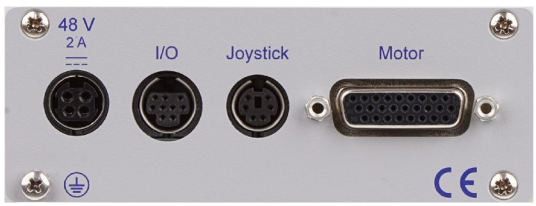

Figure 3.5: C-663.12 Mercury step controller back panel [11]

Table 3.3: Electrical parameters of the C-663.12 Mercury Step controller

Electrical parameters	**Values**
Max. output voltage	48 V
Max. output power	60 W
Current limitation per motor phase	2.5 A

The recommended ECU for this manipulation platform is the C-663.12 Mercury Step [7] shown in Figure 3.4. This ECU has a robust housing and it is powered by an external 48 V / 2 A power supply. It can drive a stepper motor in both open-loop control and closed-loop control. Its electrical parameters can be found in the Table 3.3, the motion control features are briefly listed in the Table 3.5 and the connectivity interfaces are then listed in the Table 3.4.

Table 3.4: Connectivity and operation interfaces of the C-663.12 Mercury Step controller

Connectivity and operation interfaces	/
Communication interfaces	USB, RS-232
Motor / sensor connection	HD SUB-D 26(f)
I/O lines	4 analog / digital TTL inputs 4 digital TTL outputs
Command set	PI General Command Set (GCS)
User Software	PIMikroMove
Application programming interfaces	API for C / C++ / C# and others
Manual control	Joystick, pushbutton box

The ECU supports functions such as Point-to-Point motion. This allows the platform to move to the desired point given by coordinates. Another functionality is a data recorder for high-speed tracing of the velocity, position, and position error. It also has a startup macro feature, which allows the user to customize the startup sequence to their liking. This startup sequence is then programmed into the non-volatile memory and is executed every time the ECU is switched on. All the functionality mentioned above is accessible to the user from the provided software through the use of the USB interface. Last but not least, the ECU is equipped with an internal safety circuitry and Status and Error indication LEDs. Since this ECU can only drive one axis, two of them are necessary to drive the M-971 platform.

Software and Standard Functionality

The manufacturer provides easy-to-use motion control software [5]. Once connected to the ECU by a USB, it can recognize the connected device and set the appropriate preset parameters. This software has extensive capabilities. It can be used for the most basic

Table 3.5: Motion and control features of the C-663.12 Mercury Step controller

Motion and control features	/
Number of Axes	1
Controller type	PID
Dynamics profile	Trapezoidal velocity profile
Microstep resolution	1/2048 full step
Limit switches	2x, programmable
Reference switches	1x, programmable
Encoder input	A/B quadrature
Stall detection	Motor stop when a programmable position error threshold is exceeded

functionalities, such as a point-to-point motion and reading of connected sensors and analog inputs.

Since many applications require automated motion sequences, the user can specify motion macros using the General Command Set. Another feature is the visualization of the data, which is recorded by the ECU.

For more advanced tasks and implementations into 3rd party software, it provides standardized APIs for common programming languages.

3.2 Batteries

As mentioned in the section 2, one of the parameters that set the proposed manipulation platform apart from the others is that it is self-powered by a battery. Therefore it is necessary to research battery options for this device.

The proposed manipulation platform control system is supposed to be very compact and portable. This means, that the battery that will power this device needs to be compact and lightweight as much as possible. It needs to have a decent capacity while still being able to handle the required load current of the device. The required load current is highly dependable on the used motor technology and the size of the motor. Another important factor to consider is the lifespan [12] and cost of the battery.

3.2.1 Lead Acid Battery

The lead-acid battery is a rugged and reliable technology [13]. It can deliver high current to demanding loads. On top of that, the cost is lower than most other battery technologies.

However, this type of battery works best for applications, that require few deep discharge cycles. Since the manipulation platform is meant to be used daily, which means a lot of discharge/charge cycles, it is not a great option. Another disadvantage is the relatively low specific energy, which is only 30-50 Wh/kg. That means that to get a decent capacity, the battery would be too big and heavy for a compact manipulation platform. Last but not least, it has a very slow charge rate of 0.1 C to 0.05 C (16 h charge time to get to full saturation).

3.2.2 Li-ion Battery

Li-ion batteries can deliver high capacity in a small package with low maintenance and are often used in portable applications [16].

The specific energy of this battery varies from 100 Wh/kg to 260 Wh/kg based on the used chemical compounds in the battery and its life span is often hundredths of discharge/charge cycles [15]. The recommended charging rate is 0.7 C - 1 C, which yields a 3 h charging time to get to full saturation.

Commercially available Li-ion batteries are typically packaged in a cylindrical cell that measures 18 mm in diameter and 65 mm in length [14]. This cylindrical cell is often referred to as the 18650. The 18650 has one of the lowest prices per Wh, is very reliable, and has a nominal voltage of 3.7 V. Several 18650s can easily be placed in a series-parallel combination for varying voltage, current, and capacity requirements.

The main drawbacks of a Li-ion battery are its safety and shipping constraints.

3.2.3 Ni-MH Battery

Ni-MH battery is one of the most available rechargeable batteries for consumer use [18]. It is a relatively safe battery, which is typically packaged in AA and AAA formats. Due to this, it is easy to transport, unlike a Li-ion battery.

Its specific energy is in the range of 60 Wh/kg to 120 Wh/kg, which places it somewhere between the Lead-Acid Battery and the Li-ion Battery [17]. The lifespan is between 300 to 500 discharge/charge cycles and the recommended charging rate is 0.5 C to 1 C. Batteries of this type can easily be placed in a series-parallel combination for varying voltage, current, and capacity requirements.

The downside of this battery cell is the relatively low nominal voltage of 1.2 V and the so-called memory effect, which reduces the battery capacity and requires special discharge cycles every so often to mitigate it.

3.3 Battery Charging

Since the manipulation platform control system runs on a battery, it requires its own charger, that can charge the battery safely and reliably which prolongs the battery life span [21].

Every battery technology requires a specific battery charging circuitry and algorithm. Because the Li-ion battery would be the most suitable for most designs, only the charging method for a Li-ion battery is described here.

3.3.1 Charging a Li-ion Battery

The Li-ion charger is a voltage and current limiting DC power supply that requires tight voltage tolerances [19]. Manufacturers of Li-ion cells are very strict on correct voltage levels since Li-ion cannot accept overcharge.

The ordinary Li-ion cell is typically charged to 4.20 V. The usual tolerance for the maximum voltage is ± 50 mV. Boosting the voltage of the cell increases capacity, but going beyond the specified values will stress the battery, which in turn can compromise the safety and reduce the lifespan. That is why protection circuits are included in commercially available Li-ion battery packs [20].

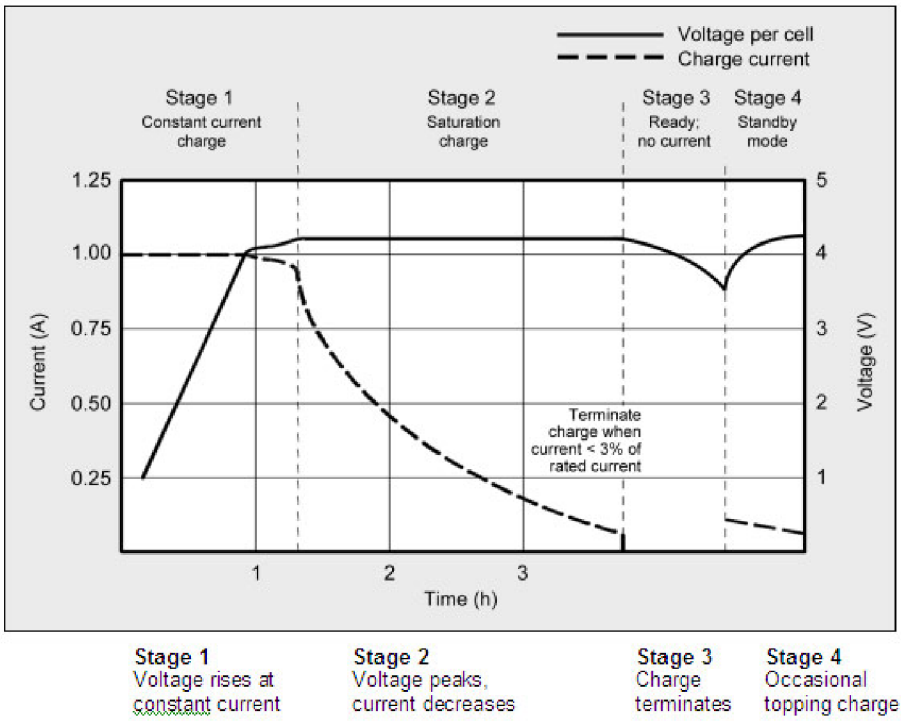

Figure 3.6: Charge stages of Li-ion battery [22]

These protection circuits feature several different protections. Mainly, they do not allow the cell to exceed the maximum allowed voltage when charging and also prohibit

it from dipping below the minimum allowed voltage during discharge. Another feature is the over-current protection, which is mostly a simple fuse or a PTC (reversible fuse). Last but not least, a balancer circuit is used in packs with multiple cells. The balancer makes sure that each cell is charged equally during the charging process.

The charging process of a Li-ion battery consists of four stages, as seen in Figure 3.6. In stage 1, a constant current source charges the battery close to its maximum charge voltage. In stage 2, which is called a saturation stage, a constant voltage source starts limiting the maximum voltage. As the constant voltage source takes over the control, the current starts falling. The battery is fully charged when the charging current falls to less than 3 % of the rated current. In stage 3 the battery is considered fully charged, but it can be seen that the voltage drops slightly after a few hours of standby. Some chargers then apply a topping charge in stage 4.

Increasing the charging current does not speed up the charging process. Although stage 1 is faster, the saturation stage will take longer accordingly. A high current charge will, however, quickly fill the battery to 70 %.

What is important to note, is that the Li-ion battery does not need to be fully charged. It is better to not charge it fully, since it stresses the battery and reduces its lifespan. Choosing a lower voltage threshold prolongs the battery lifespan but reduces run-time. Chargers for consumer products opt for the maximum capacity because an extended lifespan is perceived as less important.

Industrial chargers usually set the voltage threshold lower on purpose, to prolong the lifespan of a battery. Low-end chargers use the simplified "charge and run" method that omits the saturation stage. The Table 3.6 shows the estimated capacity after stages 1 and 2, based on the maximum voltage threshold.

Table 3.6: Typical charge characteristics of Li-ion battery [19]

Charge $[V/cell]$	**Stage 1 capacity**	**Charge time**	**Stage 2 capacity**
3.80	40%	120 *min*	65%
3.90	60%	135 *min*	75%
4.00	70%	150 *min*	80%
4.10	80%	165 *min*	90%
4.20	85%	180 *min*	100%

3.4 Wireless Control

Since the boom of Industry 4.0 and IoT, a variety of low-power wireless technology has emerged [23]. For the manipulation platform control system, the wireless communication technology must serve as a cable replacement via which it is typically driven from a PC in real-time, as mentioned in the subsection 3.1.2. The idea is that the platform would be controlled by commands in short periodical intervals.

For the communication protocol to work in real-time, it needs to be both deterministic and reliable to a certain degree [26].

Determinism here means, that the packet arrives in a pre-determined time frame. Timely data transmission is mandatory for real-time systems because the data loses its relevance after a specific time period. That is why determinism is important.

Reliability stands for the ability of the protocol, to deliver the packet of data and reduce packet loss. If too many packets are lost, the protocol is unreliable and cannot be used for industrial applications.

The main cause of having a non-deterministic behavior of the protocol is the re-transmission scheme. The re-transmission of data packets allows for higher reliability of the protocol but reduces its determinism. The clear solution is to limit the number of re-transmission per data packet. By imposing the limit, the maximum transmission delay can be determined. This in turn gives rise to packet loss. Therefore a fine balance needs to be found based on the application requirements.

3.4.1 Bluetooth

One of the main advantages of a Bluetooth solution, is its wide usability, cost, and support from many different manufacturers, devices, and systems. There are two versions of Bluetooth right now, where one of them is called Bluetooth Classic and the other is called Bluetooth Low Energy (BLE) [24]. Only BLE is introduced here, since it has substantially better parameters when it comes to battery-operated systems, such as the proposed manipulation platform control system.

Bluetooth Low Energy

BLE radio is a low-power radio that can stream data over 40 channels in the ISM frequency band. The fact that it uses the ISM band of 2.4 GHz makes it ideal for usage on the global market.

Figure 3.7: BLE modules for PCB implementation [25]

BLE employs the Adaptive-Frequency Hopping (AFH) [28] to avoid eavesdropping and interference from other devices in the ISM band. AFH is a method of transmitting

radio signals by rapidly changing the carrier frequency in a specific range - the channels. Both the receiver and transmitter know which channel will be used next and therefore they send/listen on that frequency. If any of the channels are heavily utilized by other devices, they get blacklisted and are not used until they are reliable again. Based on the latest BLE Core Specification v5.0 [27], the maximum transmission speed is 2 *Mbps*.

To set up the BLE wireless communication from the hardware standpoint, all that is necessary is a BLE USB dongle on the side of the PC and a BLE module on the ECU.

Nowadays, manufacturers offer a variety of BLE modules, that consists of a System-on-Chip (SoC) controller and a Host, which can be a part of the SoC or a standalone chip [26]. The controller handles the low-level layers of the BLE protocol stack, while the Host deals with higher layers (Figure 3.8).

Some of the modules come with an internal antenna and most of the modules have a BLE protocol stack preprogrammed. This frees the developer from the complexities of a BLE protocol stack development and RF development. The BLE module can then easily be implemented onto the ECU. For the application layer, the developer can utilize one of the official BLE GATT-Based profiles, the manufacturer's custom profile, or his own developed profile according to the specification.

The determinism and reliability of the BLE protocol depend on the used BLE protocol stack parameters as shown in [26].

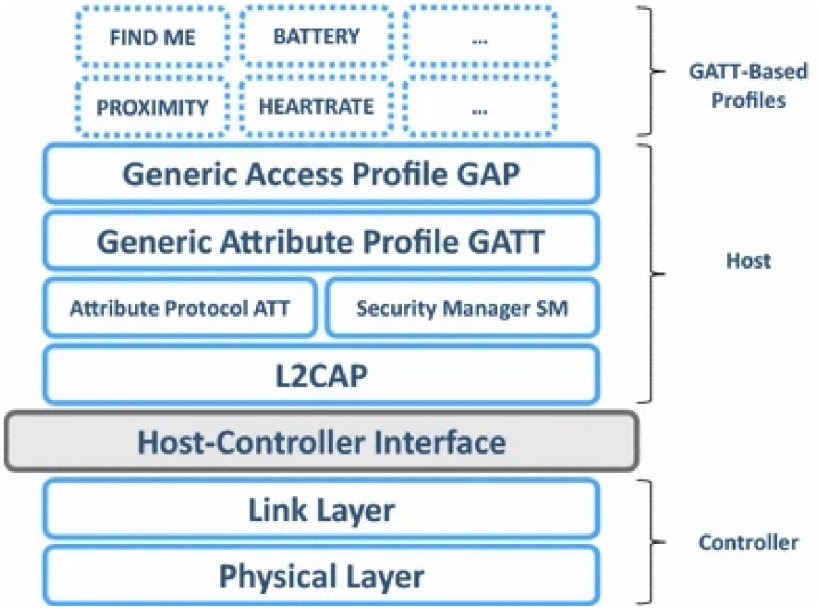

Figure 3.8: BLE protocol stack [26]

4 Electronic Control Unit Concept

This chapter deals with the concept design of an ECU for the proposed manipulation platform control system by using the knowledge from Chapter 1 and Chapter 3. The ECU is conceptualized in the Section 4.1 by defining 5 high-level functional requirements for the manipulation platform control system. The ECU Concept Design Diagram can be found in the Figure 4.1.

4.1 ECU Conceptualization

Creating a concept design diagram is very important for the design of the ECU itself. It shows the main building blocks of the ECU and therefore helps the designer navigate the whole system and its design requirements.

Since the concept of the ECU is based on the functional requirements of the manipulation platform control system, it is necessary to define them. The functional requirements are based on the research of standard technologies and control functionalities of industrial manipulation platforms in Section 3.1 and the motivation given in Chapter 2. The major functional requirements of the proposed manipulation platform control system are defined in the points below.

A: It is a compact, plug-and-play control system for a motorized manipulation platform, that can move precisely in the XY plane.

B: The control system is self-powered by a battery.

C: The system is controlled wirelessly via BLE technology from the PC application.

D: The user can set default motion parameters of the control system from the PC application.

E: The control system features status LEDs that indicate the different states of the device to the user.

Each control system functional requirement imposes a set of design requirements on the ECU, firmware, and software. In the subsections below, a detailed overview of each ECU design requirement is written.

Functional Requirement A

The ECU must reside inside of the manipulation platform, and therefore, there must be an emphasis on the miniaturization of the ECU itself. The idea is to create one PCB that provides all of the required functionality.

For the system to be plug and play, the setup must be as straightforward as possible. The user should be able to turn the system ON/OFF by a simple switch and be able to control it via the PC without any time-consuming setup processes. This means that the

ECU should be pre-programmed with the necessary default parameters for the motion and inter-connectivity of the platform.

Precise motion in the XY plane requires a set of two motors, therefore a set of two drivers is required. Each axis requires a limit switch on each end of the axis for homing purposes and safe motion control. Both the motors and the limit switches must be interfaced with the ECU via a set of connectors. Depending on the used motor technology and application requirements, external sensors such as encoders might be used as well.

Both manual control and precise point-to-point motion are expected.

Functional Requirement B

Self-powering the whole system by a battery introduces a variety of design requirements for the ECU.

First of all, the battery must reside inside the manipulation platform. The dimensions of the battery must conform to the internal dimensions of the manipulation platform. The battery's voltage, maximum load current, and capacity depend on the used motor technology and the application's dynamic motion parameters.

Once the battery is chosen, it needs to be connected to the ECU via a connector and managed according to its specifications.

The battery needs to be charged by an onboard charger. The charger requires a charging connector on the ECU and an external charging connector that is used by the user.

Safety measures, such as over-current protection, over-voltage protection, and over-heating protection must be a part of the ECU design. The ECU must also recognize when the charging cable is connected so that the system can actively block the usage of the platform during charging.

The battery's voltage and charging current must be monitored to know the state of charge of the battery at the given time.

The whole ECU needs to be optimized for efficient usage of the battery's capacity.

Functional Requirement C

Controlling the platform wirelessly from the PC via BLE imposes hardware requirements on both the PC side and the ECU side.

Desktop PCs used in the scientific setting usually do not have a BLE module on their motherboards, unlike most commercially available laptops that have it built-in. Therefore, the PC requires the use of a USB BLE Dongle. The ECU uses a BLE Module. The BLE Module must use a BLE software stack that adheres to the Bluetooth v5.0 core specification [27] so that it can be easily paired with the USB BLE Dongle. To conform to the previous plug-and-play requirement, establishing the connection link between the ECU and the PC must be as automatic as possible.

Functional Requirement D

To satisfy the functionality of setting default motion parameters, that are kept as default after a reset of the platform, a non-volatile memory must be present on the ECU.

The memory can be used for more functionality, such as saving long-term usage data of the platform, advanced battery data, manufacturing date and ID, BLE pairing key, etc. This kind of data could also prove useful in case of a malfunction of the platform. To retrieve the data for service and repair purposes, a simple service interface must be

implemented to allow direct connection of the ECU with the PC.

Functional Requirement E

The platform's states will be shown in the PC control application, however, status indication LEDs can prove invaluable, especially for the most basic of states, such as a battery state, connectivity state, and charging state.

Since the ECU is inside of the platform, the status indication LEDs would need to be brought out to the internal walls of the platform, where a hole would have to be drilled. This would vary with each hardware design of the platform. There is already a need for a hole for the ON/OFF switch and the charging connector that has to be reachable by the user on the side of the platform. Therefore, to allow easy implementation of the ECU in a variety of manipulation platforms, the ON/OFF switch features an RGB LED ring, which acts as a status indicator.

Additional Functionalities

In the section 2, one of the proposed use cases for this manipulation platform control system is in manipulation platforms in the field of computer tomography systems. In this use case, the manipulation platform is mounted on top of the rotational element of the computer tomography system.

This rotational element is mainly used for the scanning process, but sometimes it is also used to check the position of the object prior to the scanning. Since the operator does not always have the platform in his line of sight, he does not see the orientation of the platform. Once the operator uses the rotational element, the XY coordinate system of the manipulation platform rotates together with it. This makes both point-to-point control and manual control cumbersome.

To combat this issue, an Inertial Measurement Unit (IMU) is a part of the ECU concept. The idea is that the user would be able to set his default position and the PC application would show him the real-time rotation of the coordinate system of the platform.

4.2 ECU Concept Design Diagram

All the ECU design requirements are defined and summarized in Section 4.1. Ultimately, the ECU Concept Design Diagram is created. The diagram can be seen in the Figure 4.1. The concept diagram divides the high-level design requirements into functional blocks of the ECU. The ECU design Chapter 5 is logically divided by the design requirement blocks in the concept diagram.

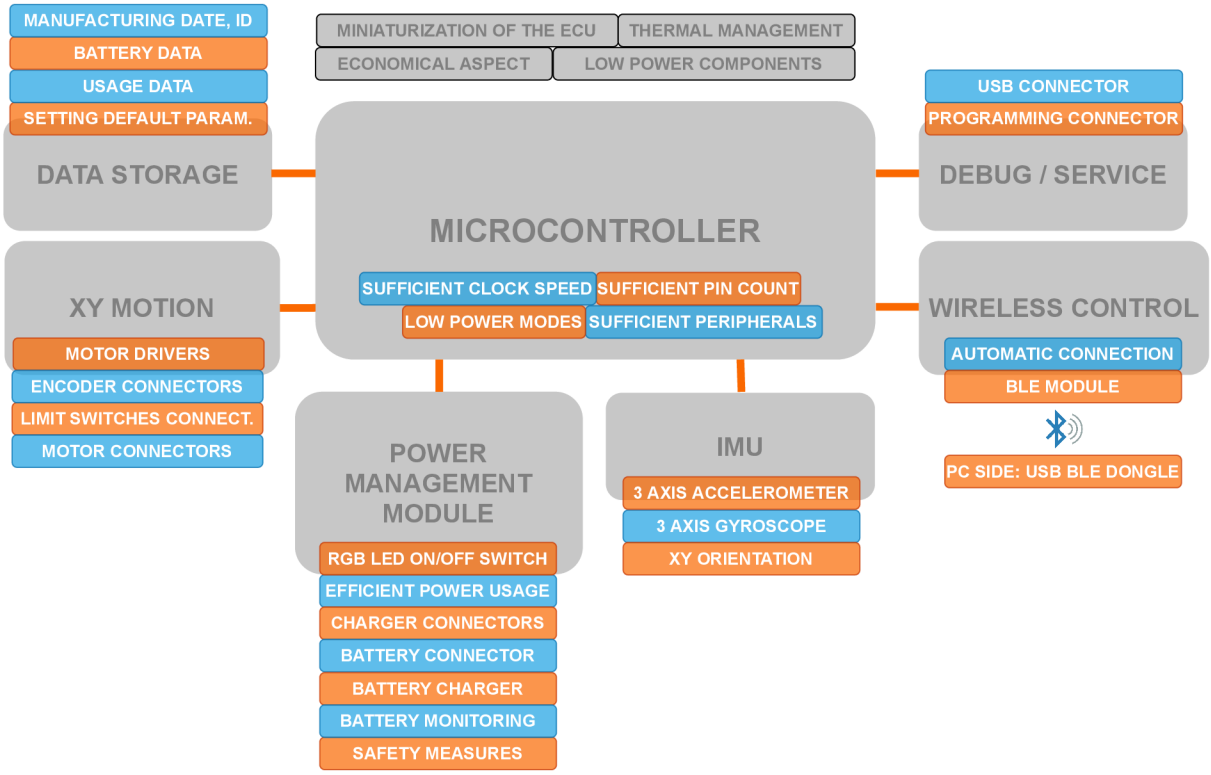

Figure 4.1: ECU Concept Design Diagram

5 Electronic Control Unit Design

This chapter deals with the systematic design of the ECU for the manipulation platform control system. Sections of the design closely follow the ECU concept diagram. The ECU design consists of the following functional blocks: XY motion, IMU, wireless control, data storage, debug and service, power management module, and microcontroller. Eventually, the ECU PCB is designed in the Section 5.9

5.1 General Requirements

The ECU must meet its general requirements, which are defined in the concept diagram. Miniaturization of the ECU is done via the usage of small SMD component packages wherever possible. The thermal management is handled by a passive cooling system designed in Section 5.9.3. The ECU also utilizes efficient components to reduce the power dissipation and increase the run-time of the battery.

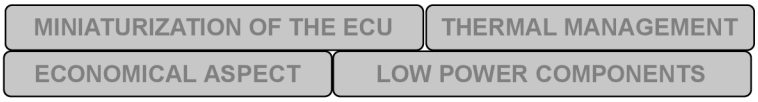

Figure 5.1: General Design Requirements Block

5.2 XY Motion

The ECU design requirements for motion are defined by the XY motion requirements block, which can be seen in the Figure 5.2.

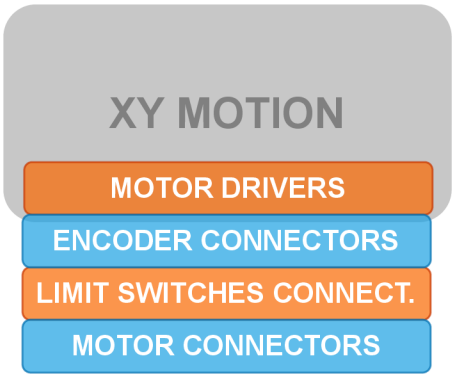

Figure 5.2: XY Motion Design Requirements Block

As mentioned in the Section 3.1, the quality of the platform motion is highly influenced not only by the mechanical design, but also by the selection of motors, motor drivers, and motion sensors. The control algorithm also plays a big part.

5.2.1 Motor Type

The motor type is not specified in the XY motion block because the ECU concept is independent of used motor technology. However, motors and their motor drivers must be chosen for the control system prototype. In the thesis of M. Remiš [31], various motor technology is described for manipulation platform usage. Eventually, a stepper motor is chosen by him for both the X and Y axis of this prototype.

5.2.2 Stepper Motor

The chosen stepper motor parameters are shown in the Table 5.1.

Table 5.1: Stepper Motor Parameters [30]

Step angle	1.8°
Number of phases	2
Rated current	1.7 A
Holding torque	560 mNm
Detent torque	24 mNm

5.2.3 Stepper Drivers

The chosen motor is a 2 phase bipolar hybrid stepper motor. These motors can be driven by two H-bridge circuits. H-bridges are switched on and off by a MOSFET gate driver

connected to the microcontroller. The microcontroller produces a specific step sequence to actuate the motor. This arrangement allows for very basic control of the stepper motor.

For more advanced driving functionality, many manufacturers offer an integrated circuit (IC) stepper driver. The IC implements the above-mentioned circuit and many others. The advantage of ICs is that they pack a lot of functionality into a small package, which is great for keeping the ECU as small as possible.

To keep the overall development time for both the ECU and the firmware to a minimum, a decision is made to use the IC stepper driver. Since M. Remiš is in charge of the motion algorithm, one of his goals is to choose the stepper driver IC.

Trinamic TMC2130

The chosen stepper driver is the TMC2130 from the company Trinamic. It is offered in TQFP (Figure 5.3) and QFN (Figure 5.4) packages. Both packages offer the same functionality, except for the maximum RMS current capability. The QFN package offers the maximum RMS current of 1.2 A while the TQFP package offers the slightly higher 1.4 A. The QFN package's current capabilities would be sufficient for the chosen stepper motor since the motor will not be driven by its maximum current. It would also be beneficial to use the QFN package to keep the ECU size as small as possible. However, during the design phase, it is not available due to the global component shortage. Therefore, the TQFP package is used for the ECU.

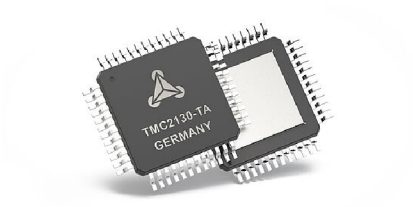

Figure 5.3: Trinamic TMC2130, TQFP Package [32]

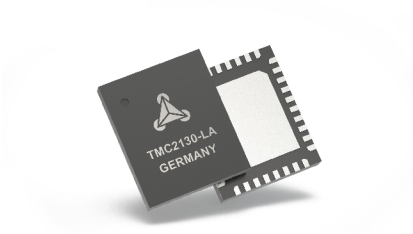

Figure 5.4: Trinamic TMC2130, QFN Package [33]

The stepper driver IC implements a standard STEP/DIR interface for motion control and an SPI interface for configuration and diagnostics. It uses integrated power MOSFETs to drive both phase coils of the motor. The high-level interface diagram can be seen in the Figure 5.5

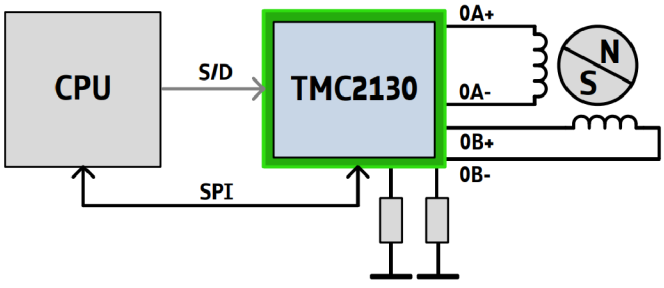

Figure 5.5: TMC2130 Interface Diagram [34]

Using the SPI control, it is possible to set the maximum current limit and micro-step

resolution based on the need of an application. This feature allows the driver to be used for a variety of stepper motors and manipulation platform sizes.

The ECU implements two TMC2130, one for each axis. The electrical schematic of both drivers is done according to the manufacturer's recommendations in [34]. Schematics can be found in appendix 6, 7, and 8.

What is important to note, is that the IC requires three different power buses. 3.3 V for the control interfaces, 5 V for the internal analog circuitry, and the main power supply for powering the motor, which in this case is the battery. The Subsection 5.7.9 deals with power bus design. The IC dissipates substantial power when used with the maximum current setting. The thermal management of the IC is done in the Subsection 5.9.3.

Figure 5.6: PicoBlade 4 Pin Connector [35]

Connectors often use a significant amount of space on the printed circuit board (PCB). To minimize the connector area as much as possible, small footprint connectors are used. Both motors are connected to the ECU via two 4-pin PicoBlade connectors (Figure 5.6) from the company Molex.

5.2.4 Limit switches

Each axis must have a limit switch at the start of an axis and the end of an axis. Limit switches are often simple true or false sensors, that are used for stopping the motor when it tries to go out of bounds. They can be either hardwired switches or software switches. Hardwired switches disconnect the power to the motor once they detect that the motor is out of bounds. Software switches only indicate their state to the controller. The controller has to check the state of the limit switch whenever it tries to drive the motor.

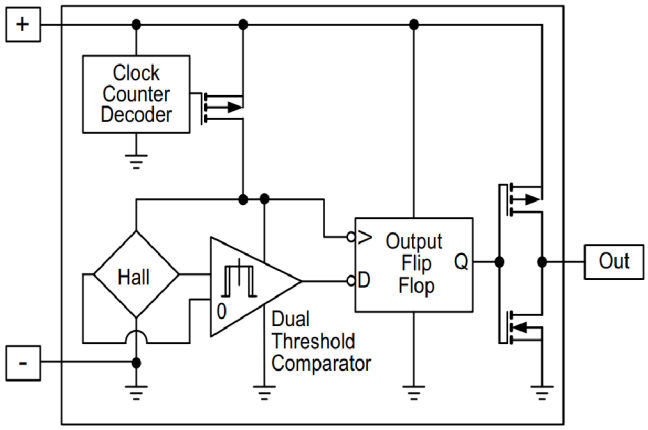

Figure 5.7: SL353LT Circuit Diagram [36]

For this prototype, small and simple software limit switches are designed using a hall omnipolar sensor IC SL353LT [36]. The sensor has three pins: power, ground, and digital output as can be seen on the electrical diagram in the Figure 5.7. Whenever there is a magnetic field in the proximity of the sensor, it outputs a log. 0 instead of a log. 1.

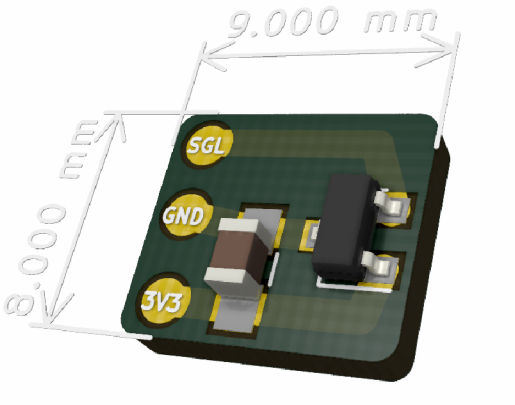

Figure 5.8: Hall Limit Switch

A low-cost, 1-layer PCB is designed for the sensor (appendix 24). The electrical schematic can be found in appendix 23. The 3D model of the designed limit switch is shown in the Figure 5.8. These limit switches are very compact and can be fitted to the start and end of each axis. The motor carriage must include a permanent magnet. Whenever the motor carriage gets to the proximity of the limit switch, the magnetic field created by the permanent magnet triggers the limit switch.

Four limit switches are required for the design. On the limit switch side, three cables of sufficient length are soldered onto the exposed pads of each limit switch. On the ECU side, the PicoBlade connector is used once again, this time with 12 pins to house all the limit switches. The electrical schematic of the connector can be found in appendix 9.

5.2.5 Encoders

Absolute rotary encoders, which are chosen by M. Remiš in his thesis, can be seen in the Figure 5.9. The main idea behind using absolute encoders is to remove the necessity of homing after each reset of the manipulation platform. Using an encoder also opens up the possibility of closed-loop control for more demanding applications.

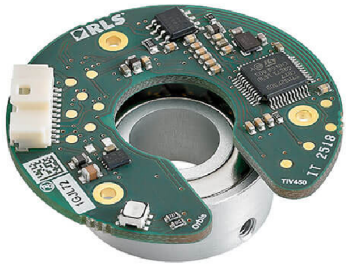

Figure 5.9: Absolute Rotary Encoder Orbis™ [37]

Two Orbis encoders from the company RLS are used, one for each axis. The encoder communicates via the SPI interface and uses a total of 6 pins. Both encoders are connected to a single 12-pin PicoBlade connector in order to save space. The electrical schematic can be found in appendix 3.

5.3 Inertial Measurement Unit (IMU)

The Inertial Measurement Unit is used to keep track of the orientation of the local coordinate system of the manipulation platform inside the CT system. A more detailed explanation of why is it necessary is given in the Subsection 4.1.

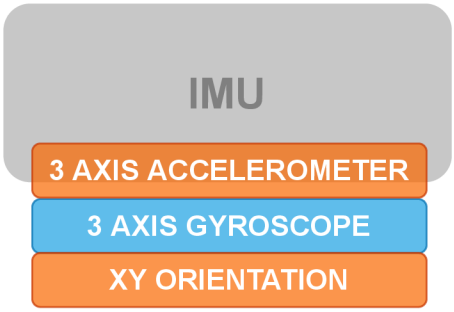

Figure 5.10: IMU Design Requirements Block

The IMU must be a low-power device that features a 3-axis gyroscope, digital interface (SPI or I2C), and sufficient sampling frequency.

InvenSense ICM-20789

The ICM-20789 from Ivensense is an integrated 6-axis inertial device, that combines a 3-axis accelerometer, 3-axis gyroscope, and a precise pressure sensor into a 24-pin LGA package. It is a very precise, temperature stable, low-power IMU. The pressure sensor is not wired and the accelerometer is not necessary, but due to the global component shortage, there is no alternative at the time of design.

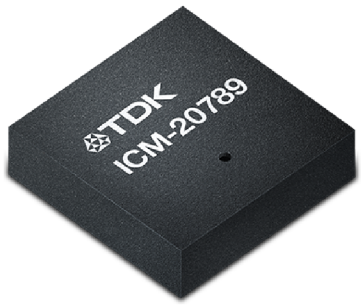

Figure 5.11: 6-Axis IMU, IvenSense ICM-20789 [39]

The ICM-20789 comes in a very small 4x4 mm package (Figure 5.11). The accelerometer has a programmable resolution, up to ± 16 g and the gyroscope has a programmable resolution up to ± 2000 dps. Both the gyroscope and the accelerometer can sample at a maximum of 8 KHz, which is sufficient for this application. It also features programmable digital filters and a plethora of other functionalities.

It requires to be powered by a 1.8 V bus, and also its I2C digital interface works on the 1.8 V level. Interfacing would usually be problematic and require additional circuitry in the form of logic level shifters since most microcontrollers nowadays use the 3.3 V for both power and digital interfaces. However, a better solution to this problem is found

and explained in the Section 5.8.

The electrical schematic is designed according to the recommendations in the manufacturer's datasheet [38] and can be found in appendix 12. The I2C data and clock lines are fitted with standard 2.2 $k\Omega$ pull-up resistors.

5.4 Wireless Control

For the wireless control of the manipulation platform, the BLE wireless interface is chosen. It is low cost, low power, adaptable, and relatively easy to implement.

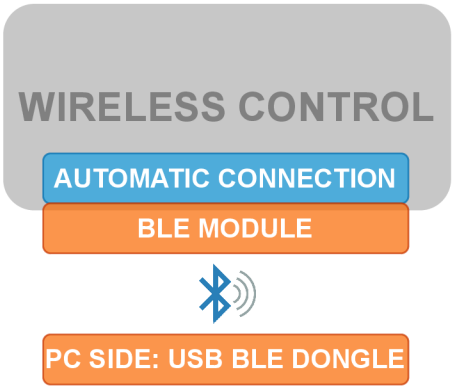

Figure 5.12: Wireless Control Design Requirements Block

A communication protocol that uses special commands for the manipulation platform is created as a part of M. Remiš's thesis [31]. This communication protocol uses the BLE as a raw data pipe, that allows the wireless transmission and reception of said commands. The protocol works in the following way.

The command packet is periodically sent from the PC software to the ECU. M. Remiš empirically determined that a period of 100 ms is sufficient for the real-time human control of a manipulation platform. The ECU replies as soon as possible with its own special echo packet back to the PC. Both the command packet and the echo packet size can vary up to 48 *bytes*. Therefore, the required data throughput of the BLE module and BLE dongle is 960 $bytes/s$.

5.4.1 BLE Module

The ECU requires a BLE module that has a small form factor and low energy consumption. The module must also have castellated holes so that it can be easily soldered onto the ECU. The transmission speed of the module needs to be more than 960 $bytes/s$ and the antenna range of the BLE module should be at least 5 m.

BM70

The chosen BLE module is the BM70 (Figure 5.13), from the company Microchip, which is built around an IS1870 System on Chip (SoC). The SoC comes with a preprogrammed BLE protocol stack, power management subsystem, 2.4 GHz transceiver, and RF power amplifier. The BLE stack of the device is qualified for the Bluetooth Core Specification v5.0 [27], which means it adheres to the BLE standard. The version that is used on the ECU also features an onboard chip antenna that is certified for use in most countries.

Figure 5.13: BLE Module BM70 [40]

The datasheet [40] of the module states the following parameters. The average current consumption of the module with default parameters is 3.3 mA for transmission and 3.2 mA for the reception. In this mode, the data rate is approximately 1.05 kB/s and the antenna range on this module is said to be up to 50 m.

The electrical schematic of the BM70 is designed by using the manufacturer's recommendations in the datasheet [40]. The schematic can be found in appendix 10. The module is powered by 3.3 V. It is interfaced with the ECU via a UART, status indication pins, and configuration pins. The module features two modes of operation. One is called the auto-pattern mode profile and the other is called the manual mode profile.

In the auto-pattern mode, the BM70 is automatically set up with the default parameters of the BLE protocol stack. Once powered, it automatically starts advertising its presence via advertising packets. When the PC's BLE dongle pairs with the device, it can be set up to start using the so-called "Transparent UART" BLE data service, which acts as a raw data pipe between the PC and the ECU. Every command packet that is received by the BM70 is automatically transmitted via UART to the microcontroller. When the microcontroller wants to transmit the echo packet, it needs to send the packet via UART to the BM70. The BM70 then automatically transmits the packet to the PC's BLE dongle. The internal layers of the BLE stack also handle the re-transmission in case of packet corruption.

If the auto-pattern mode is not sufficient for the application and needs refinement, the manual mode can be used. In the manual mode, everything needs to be done manually and the BM70 needs to be commanded over UART by a specific command set. Various parameters of the BLE can be altered and a whole new BLE GATT profile can be created. It might be beneficial to use the manual mode in the future, however, for now, it is beyond the scope of this prototype.

5.4.2 BLE USB Dongle

The PC BLE functionality can be added via a BLE USB dongle. The BLE USB dongle needs to have a sufficient antenna range and Windows 10 compatible drivers. In case there is an issue with the antenna range, a USB extension cable can be used to get the BLE USB dongle closer to the manipulation platform.

ASUS USB-BT400

This commercially available USB dongle is chosen because it has been tested before with other BLE modules. It does have Windows 10 compatible drivers and its antenna range is around 10 m.

Figure 5.14: BLE USB Dongle: ASUS USB-BT400 [41]

5.5 Data Storage

The non-volatile data storage's most important parameters are its memory size, write and read speeds, and the number of read/write cycles.

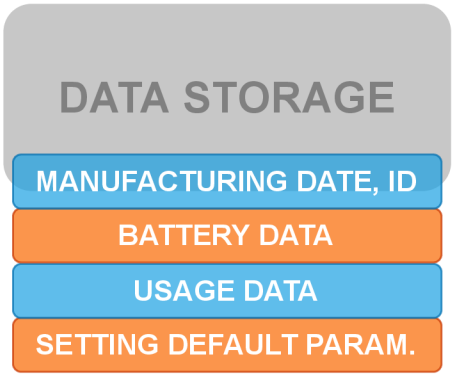

Figure 5.15: Data Storage Design Requirements Block

As mentioned in Section 3.1, manipulation platform control systems use the non-volatile data storage for storing important manufacturing parameters and allowing the user to set desired default parameters of the platform, such as axis velocity and axis acceleration. However, in the case of the proposed platform, another mentioned use in the Section 4.1 could be the battery data storage, which would allow for an advanced state of life and state of charge battery monitoring algorithm. Developing the advanced battery monitoring algorithm is a topic for future development of the project.

Since this is a prototype, it is important to design the data storage as robust as possible, so that it can be used for the development of future ideas as well.

Therefore, the requirements for the data storage are sufficient memory size, a fast digital SPI interface for fast write and read functionality, and an adequate number of read/write cycles.

5.5.1 FRAM Non-Volatile Memory

The ferroelectric random access memory (FRAM) technology is chosen. It performs write operations at bus speed. There are no delays or system overhead as is the case with flash memory or an EEPROM. Another advantage of the FRAM memory is its very high number of read/write cycles. This allows not only for simple storage of manufacturing date and ID but also for more complex functionality that might be developed in the future.

FM25CL64B-DG

The chosen FRAM IC features 10^{14} read/write cycles, up to 20 MHz SPI interface, and a $64Kbit$ of memory. It is a low-power device, which uses only 3 mA at maximum clock speed and 0.2 mA at standby. It is offered in a SOIC 8 pin package, which measures only 6 mm x 5 mm. It also offers multiple write protection functionalities. The electrical schematic is designed according to the recommendations in the manufacturer's datasheet [42]. The schematic can be found in appendix 5.

5.6 Debug and Service

The programming connector can be used for uploading the firmware to the microcontroller and for debugging, testing, and verification purposes during the development process.

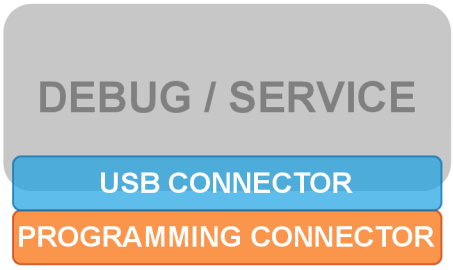

Figure 5.16: Debug and Service Design Requirements Block

To program and debug the ECU via the programming connector, an additional module called the programmer must be used between the PC and the programming connector. This is fine for the developer, but it would be inconvenient for the user to have his own programmer for the purpose of a direct PC connection.

That is why the ECU also features a service connector. Using the service connector, the user can directly interface the PC with the manipulation platform, as can be seen in the Figure 5.17.

5.6.1 USB Service Connector

The USB interface is used here because it is a standard interface in PCs and its implementation is relatively simple on the ECU side. A micro-USB connector is used together

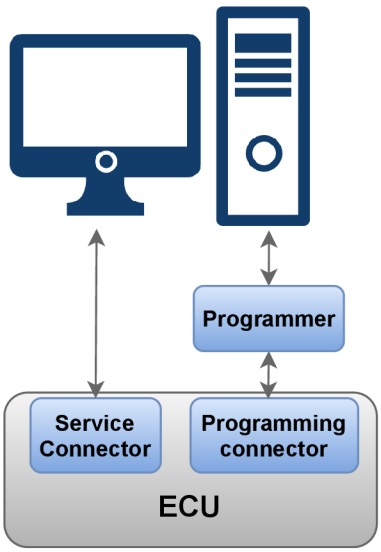

Figure 5.17: Service and Programming Connector Interface

with an ESD protection IC. Using the USB interface is also a great choice for future development because there are microcontrollers that implement a Device Firmware Upgrade (DFU) protocol through the USB interface. The DFU can be used for upgrading the firmware of the ECU without the need for a programmer.

Therefore, if properly set up, the idea is that the user would be able to download new firmware with bug fixes or new functionalities and upload it into the ECU via a USB cable and the manipulation platform's control software. The electrical schematic of the USB interface can be found in appendix 15 and 16.

5.6.2 Debug Connector

The pin count of the connector depends on the microcontroller technology and its programming and debugging interface. In the Section 5.8 it can be seen that the chosen microcontroller is an STM32476 microcontroller, made by ST. This microcontroller can be programmed via several interfaces. The chosen interface for this ECU is the Serial Wire Debug (SWD). The SWD interface requires a minimum of 3 pins.

However, for the sake of testing and verification, UART and test pins are added to the debug connector for a total of 10 pins. Therefore, a 10-pin PicoBlade connector is used. The electrical schematic of the debug connector can be found in appendix 16.

5.7 Power Management Module

The power management module (PMM) manages the battery, power buses, the smart usage of peripherals, power safety measures, and others. Its design consists of three electrical schematics. The first one is the main PMM schematic found in the Figure 5.24. The second one is the battery charger schematic found in the Figure 5.22. The third schematic that shows the peripheral power switch design is shown in appendix 15.

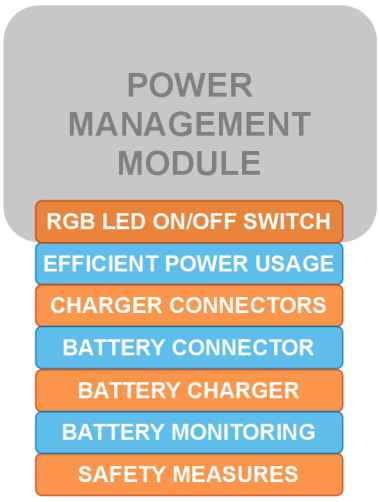

Figure 5.18: Power Management Module Design Requirements Block

5.7.1 Battery

The battery choice is highly influenced by the size of the manipulation platform, used motor technology, and maximum required velocity and acceleration of the axes. For this prototype, Li-ion battery technology is chosen due to its compact size and high specific energy. The chosen battery pack is the CL-18650-29E4S2P. This is a standard Li-ion battery pack with eight 18650 cells in a 4S2P parallel-series combination. The battery pack features internal protection and balancing circuit, that balances each cell and monitors the overvoltage of each cell and under voltage of each cell. It also has over-current protection in case of a short circuit condition. The important battery parameters are listed in the Table 5.2.

Table 5.2: Parameters of CL-18650-29E4S2P Battery Pack [43]

Nominal Voltage	14.6 V
Capacity	5540 mAh
Max Charge Voltage	16.8 V
Max Continous Discharge Current	3.3 A

The nominal voltage is chosen with respect to the stepper motor technology. With higher voltages, stepper motors have a much better torque-speed characteristic at the cost

of slightly higher iron losses of the motor windings [44].

The maximum continuous discharge current of the battery is sufficient even for both stepper drivers running at full current. The battery is connected to the ECU via a 2-pin PicoBlade connector.

5.7.2 Battery Charger Requirements

The charging of the manipulation platform from the user's point of view should be as convenient as charging a phone or a laptop. The user is only provided with an AC/DC adapter, that plugs into the power grid on one side and the manipulation platform on the other side. The charging should happen automatically, with the charger onboard the ECU managing all the necessities in conjunction with the microcontroller. The Figure 5.19 shows the arrangement of the charging concept.

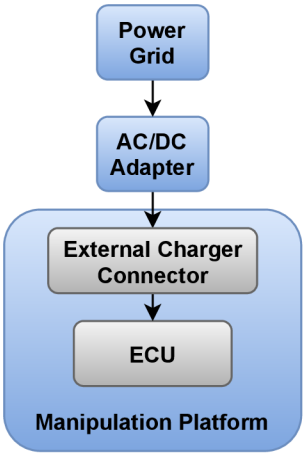

Figure 5.19: Charger Connection Diagram

From the ECU point of view, the charger must be a compact CC/CV switch-mode power supply, that is able to conform to the tight dimensional requirements of the ECU. Because the battery pack size and therefore capacity can change based on the size of the manipulation platform, the charger design must be made in a way, that can be easily adapted to the application. The adaptability can be either via robust design or via a few interchangeable components.

The maximum battery charging voltage V_{BAT} is designed based on the battery parameters from the Table 5.2 and the information from the Section 3.3, which shows that lowering the maximum charging voltage is beneficial for the lifespan of the battery.

The recommended charging current of the chosen battery is 2.75 A. However, lowering the maximum charging current allows the charger to be used with smaller battery packs, that have no parallel cells, at a cost of slightly longer charge times. These packs have the same maximum voltage but half the capacity and therefore require lower charging currents for increased lifespans. This overall increases the robustness of the ECU, which allows it to be used in various platform sizes. The electrical design requirements of the charger are listed in the Table 5.3.

5.7.3 DC/DC Converter Topology Choice

Because the charger is powered from the grid using an AC/DC adapter, which gives it easy access to DC voltage that is higher than the maximum battery voltage, the most straightforward design choice is to use the DC/DC buck converter topology. The buck converter is used for stepping down the DC voltage level. It is often used for efficient, small-area designs. The high efficiency of the DC/DC converter allows for higher currents than a standard linear regulator due to lower heat dissipation.

The most efficient DC/DC buck converter topology is the NMOS/NMOS synchronous topology. It uses NMOS switches for both the high side and low side switching, which further increases the topology's efficiency. This topology is used for the design of the battery charger.

Two main building blocks of the buck converter's circuit are the controller and the power stage. In Voltage Mode Control (VMC), the controller regulates the output voltage by employing a voltage feedback loop. In Current Mode Control (CMC), the controller regulates the output current by measuring the voltage across a shunt resistor. The measured voltage is then used for the current feedback loop. Both feedback loops are utilized for the constant current / constant voltage (CC/CV) battery charger design. A simplified diagram of the whole topology is shown in the Figure 5.20

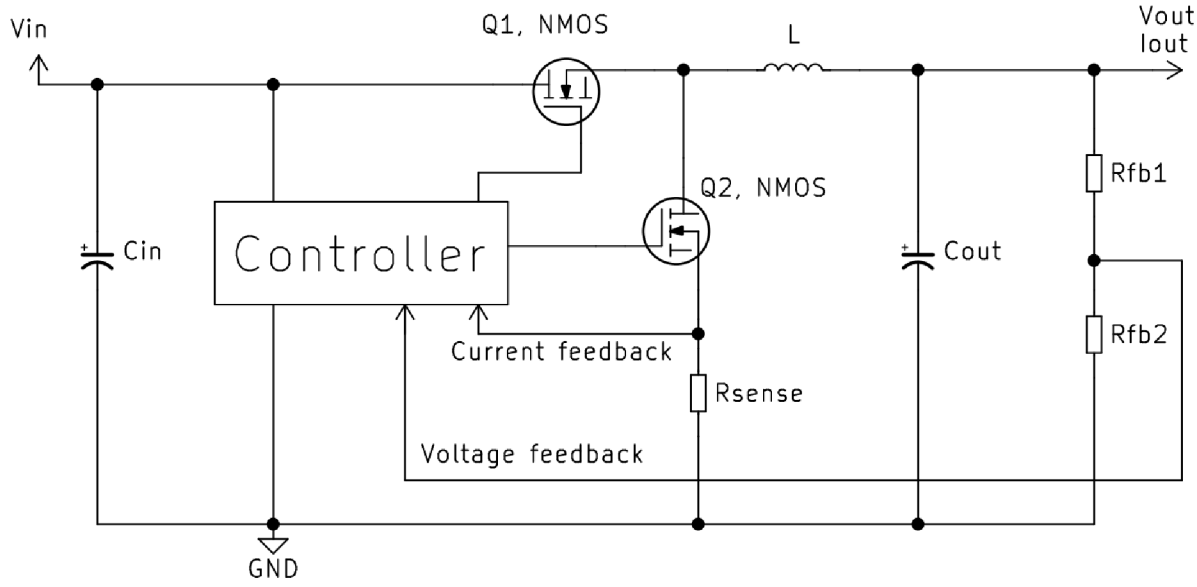

Figure 5.20: Simplified Diagram of the NMOS/NMOS Synchronous DC/DC Buck Converter with CC/CV Regulation

5.7.4 DC/DC Converter Controller Choice

To minimize the controller's area and development time, an integrated circuit solution is used. The chosen controller IC is the Texas Instruments LM5117 NMOS/NMOS Synchronous Buck Controller.

The LM5117's main features are a programmable CMC limit and programmable VMC limit, which makes it ideal for the Li-ion CC/CV battery charger. It has a wide input range, robust MOSFET gate drivers, adaptive dead-time control to avoid cross con-

duction, programmable operating frequency up to 750 kHz, diode emulation mode for increased efficiency during the light load operation, and more functionalities, that are explored in the following design sections.

5.7.5 Battery Charger Circuit Design

Commercially available AC/DC adapter with 24 V / 2.5 A output is used for the charger's input voltage V_{in}. A standard, barrel connector is used for the external adapter connector. To interface the external charger connector to the ECU, the ECU is fitted with a 2-pin PicoBlade connector.

Table 5.3: Battery Charger: Electrical Design Requirements

Maximum Battery Charging Voltage $V_{BAT(MAX)}$	16.6 V
Maximum Battery Charging Current $I_{OUT(MAX)}$	2.2 A
Input Voltage V_{IN}	24 V
Maximum Output Voltage $V_{OUT(MAX)}$	16.85 V

The converter's maximum output voltage $V_{OUT(MAX)}$ is higher than the maximum battery charging voltage $V_{BAT(MAX)}$ because a low leakage Schottky diode with a forward voltage drop of 0.25 V is used on the converter's output. The diode prohibits the battery voltage from affecting the converter when V_{in} is not present or when the converter is turned off.

Switching Frequency

The first design step is to choose the switching frequency f_{SW} of the controller, which is programmed by an external resistor R_T. The higher the frequency, the smaller the power stage inductor and output capacitor have to be. The tradeoffs are higher NMOS switching losses and gate driver losses. However, the maximum switching frequency is limited by the maximum duty cycle, which is limited by the high-side NMOS minimum off-time. The maximum duty cycle D_{MAX} of this design is calculated in the Equation 5.1.

$$D_{MAX} = \frac{V_{IN}}{V_{OUT}} = \frac{16.85V}{24V} = 0.70 \tag{5.1}$$

To keep some margin, the switching frequency f_{SW} is chosen as 500 kHz and the value of R_T is calculated according to the manufacturer's datasheet.

Power Stage Inductor

The inductance L of the inductor is calculated by using the Equation 5.2, which is provided in the manufacturer's datasheet [45]. The inductance value directly influences the peak-to-peak current $I_{PP(MAX)}$ and therefore dictates the size of the output capacitor which has to smooth out the ripple voltage on the output. To also keep a good balance of the inductor copper losses, core losses, and its size, the $I_{PP(MAX)}$ is chosen as 15 % of the I_{OUT}. The inductor is a major power dissipation element of the design and therefore its

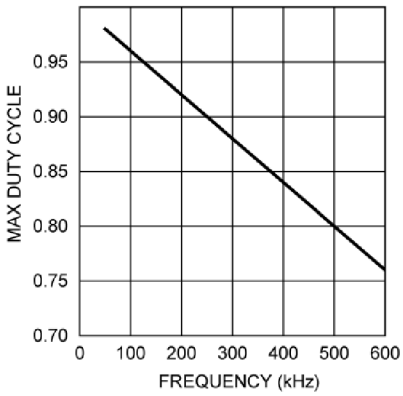

Figure 5.21: Maximum Duty Cycle vs Switching Frequency [45]

thermal management is discussed in 5.9.3. An inductor with the closest standard value of 33 μH and a high enough saturation current is used.

$$L = \frac{V_{OUT}}{I_{PP(MAX)} \cdot f_{SW}} \cdot (1 - \frac{V_{OUT}}{V_{IN}}) = \frac{16.85V}{2.2A \cdot 15\% \cdot 500kHz} \cdot (1 - \frac{16.85V}{24}) = 33.5\mu H \quad (5.2)$$

NMOS Switches

NMOS switches' drain-to-source voltage rating V_{DS} should be at least twice the input voltage V_{IN}. To reduce the amount of power that is being dissipated during the CC charging stage ($I_{OUT} = I_{OUT(MAX)}$), the drain-source resistance $R_{DS(on)}$ of the NMOS must be kept to a minimum. Generally, bigger NMOS packages have lower $R_{DS(on)}$ value. Therefore a balance between size and efficiency must be found. This is achieved by utilization of small NMOS devices in a SOT-23 package, that has a sufficiently low $R_{DS(on)}$. The chosen NMOS device for both switches is the SQ2362ES. Its parameters are listed in the Table 5.4. Power dissipation analysis of the chosen NMOS switch and the controller is conducted below.

Table 5.4: SQ2362ES Parameters [46]

V_{DS}	60 V
$R_{DS(on)}$ at $V_{GS} = 10\ V$	0.068 Ω
V_{GS}	$\pm$20 V
Q_G	7.5 nC

Gate charging losses P_{GC} result from the current driving the gate capacitance Q_G. The power dissipation happens inside the controller's gate drives and it is estimated by the Equation 5.3, which is provided in the datasheet [45]. As it can be seen, the gate charging losses P_{GC} are relatively low due to the low gate capacitance Q_G of the NMOS devices. The controller will heat up mostly due to the proximity of the power stage inductor and NMOS switches. The thermal management design of the controller is done

in the Subsection 5.9.3.

$$P_{GC} = 2 \cdot V_{VCC} \cdot Q_G \cdot f_{SW} = 2 \cdot 7.5V \cdot 7.5nC \cdot 500kHz = 0.06W \tag{5.3}$$

The dissipated power of an NMOS device P_D is a sum of conduction losses P_{DC} and switching losses P_{SW}. Using the equations provided in the controller's datasheet [45], $P_{DC(High-Side)}$ is calculated in the Equation 5.5 and $P_{DC(Low-Side)}$ in the Equation 5.6. The $P_{SW(Low-Side)}$ is negligible because of the body diode [29], therefore only the $P_{SW(High-Side)}$ is calculated in the Equation 5.7. The total dissipated power of the high-side NMOS $P_{D(High-Side)}$ is 0.76 W and the total dissipated power of the low-side NMOS $P_{D(Low-Side)}$ is 0.15 W.

It is difficult to calculate the junction temperature of each NMOS device because the designed PCB has very different parameters than the one which is used for the measurement of the thermal resistance ratings in the NMOS datasheet [46]. Past empirical evidence suggests that the chosen package should not have an issue dissipating the determined amount of energy. However, to increase the safety margin of the design, the Subsection 5.9.3 deals with the thermal management of the converter's power stage.

$$\begin{aligned} P_{DC(High-Side)} &= D \cdot I^2_{OUT(MAX)} \cdot R_{DS(on),100°C} \qquad (5.4) \\ &= 0.70 \cdot 2.2^2 A \cdot 0.105\Omega = 0.36W \end{aligned}$$

$$\begin{aligned} P_{DC(Low-Side)} &= (1-D) \cdot I^2_{OUT(MAX)} \cdot R_{DS(on),100°C} \qquad (5.5) \\ &= 0.30 \cdot 2.2^2 A \cdot 0.105\Omega = 0.15W \end{aligned}$$

$$\begin{aligned} P_{SW(High-Side)} &= \frac{1}{4} \cdot V_{IN} \cdot I_{OUT(MAX)} \cdot (t_{rise} + t_{fall}) \cdot f_{SW} \qquad (5.6) \\ &= \frac{1}{4} \cdot 24V \cdot 2.2A \cdot (30ns + 30ns) \cdot 500kHz = 0.40W \end{aligned}$$

Current Limiting

The controller has three current limiting options. For the required CC operation, cycle-by-cycle current limiting is used. That means that when the controller senses that the current has reached the maximum allowed current, it terminates the present cycle and waits until the current decays below the limit before continuing operation.

The value of the current sense resistor determines the output current limit of the converter. For the desired maximum battery charging current $I_{OUT(MAX)} = 2.2A$, the current sense resistor R_S is calculated to be 39 $m\Omega$, by using the equation provided in the controller's datasheet [45]. A temperature stable, 0.1% precision resistor with a sufficient power rating is used.

Voltage Limiting

The converter's maximum output voltage $V_{OUT(MAX)}$ is set by voltage divider resistors R_{FB1} and R_{FB2}. Using the provided formulas in the controller's datasheet [45], the values of the voltage divider resistors are determined. The closest standard values of $R_{FB1} = 1\ k\Omega$ and $R_{FB2} = 50\ \Omega$ are used. Using temperature stable, 0.1 % precision resistors, the converter's output voltage limit should be 16.80±0.03 V and the maximum battery charging voltage should be 16.55±0.03 V. This is sufficiently close to the design requirement of 16.60 V.

Battery Charger Electrical Schematic

Bootstrap circuit, input capacitor, output capacitor, compensation network, current ramp emulation, and other minor circuitry is designed by following the recommendations of the controller's datasheet [45]. The charger is designed with adaptability in mind. Its output voltage can be lowered by replacing only several resistor values. The lower output voltage is useful for very small manipulation platforms that can not fit enough battery cells in series to reach the charger's design value of $V_{BAT(MAX)}$. The designed electrical schematic of the battery charger can be found in the Figure 5.22.

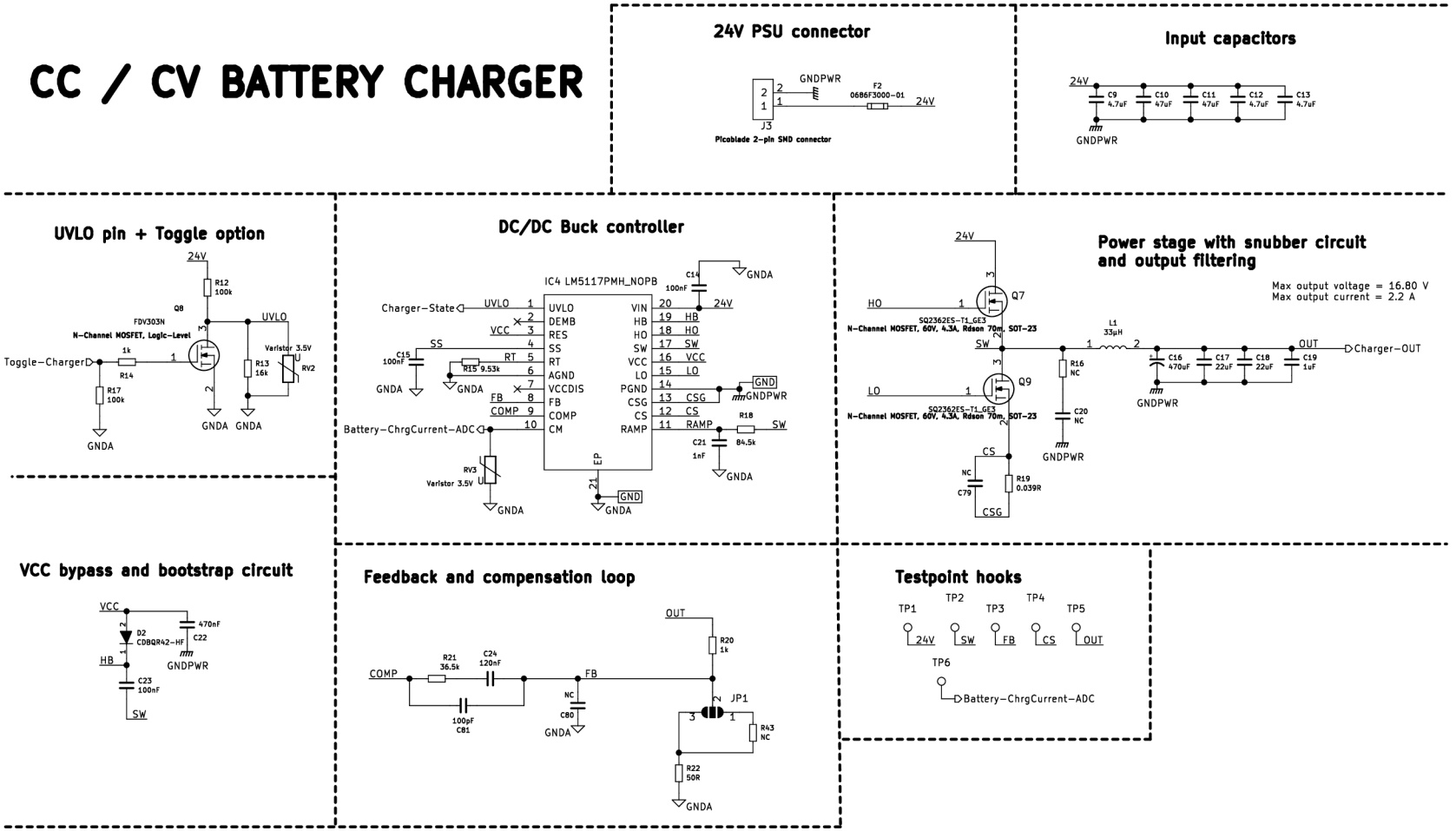

Figure 5.22: CC / CV Battery Charger Electrical Schematic

5.7.6 Battery Monitoring

During the charging and discharging cycles of the battery's lifespan, the battery's parameters must be monitored. The parameters are monitored to estimate the state of charge and to ensure its safety and longevity. For the most basic battery state of charge estimation, the battery's voltage and charging current are monitored.

Battery Voltage

The battery voltage is measured by an analog-digital converter (ADC) with a 12-bit resolution, which is a part of the microcontroller. The reference voltage V_{REF} that is used for the ADC is internally generated by the microcontroller and its value is 2.5 V. A voltage divider with resistors R_1, R_2 is employed to scale the battery's voltage down to the ADC range. To avoid draining the battery, the total resistance of the divider must be kept high. R_1 is set as 49.9 $k\Omega$. The minimum recommended battery voltage $V_{BAT(MIN)}$ is 12.00 V. The maximum battery charging voltage $V_{BAT(MAX)}$ is determined in Subsection 5.7.5 and equals 16.58 V. The maximum value of R_2 is determined via the Equation 5.7.

$$R_{2(MAX)} = \frac{R_1 \cdot V_{REF}}{V_{BAT(MAX)} - V_{REF}} = \frac{49.9k\Omega \cdot 2.5V}{16.58V - 2.5V} = 8.86k\Omega \tag{5.7}$$

To make sure the ADC measurement is not getting saturated above the V_{REF}, the value of the resistor R_2 is reduced to a standard value of 8.25 $k\Omega$. Both resistors are temperature stable precision resistors with 0.1% tolerance. With the new R_2 value, the $V_{BAT(MIN)}$ and $V_{BAT(MAX)}$ should be measured by the ADC as shown in the Table 5.5.

Table 5.5: Battery Voltage vs ADC Measurement

/	V_{BAT}	ADC measurement
MIN	12.00 V	1.70 V
MAX	16.58 V	2.35 V

Battery Charging Current

The charging current measurement design is very straightforward. The DC/DC buck controller features a Current Monitor (CM) output. The CM output voltage V_{CM} is proportional to the charging current I_{OUT} as shown in the Equation 5.8, which is provided in [45]. R_S is the current sense resistor. The V_{CM} is measured by using the microcontroller's ADC.

$$V_{CM} = (I_{PEAK} + I_{VALLEY}) \cdot R_S \cdot 10 \tag{5.8}$$

5.7.7 Safety Features

The power management module also implements the over current, over-voltage, under-voltage, and overheating safety features. Basic protections are automatically triggered,

while the more advanced protections require a firmware implementation.

Blocking Mode

Additional circuitry, that allows the microcontroller to check for external cable connections is added. Whenever it detects the connection of the USB service connector interface or whenever the user plugs in the AC/DC adapter to charge the device, the microcontroller can sense it and can react accordingly. For example, when the user plugs in the charger, the microcontroller blocks the XY motion, which prohibits the user from operating the manipulation platform during battery charging.

Over Current Protection

The overcurrent protection of the charger is handled by measuring the charging current I_{OUT}. When the measured current is higher than the $I_{OUT(MAX)}$, the charger can be turned off via a microcontroller GPIO pin.

Fuses are used for additional overcurrent protection. One is used for the charger input V_{IN} and the other for the battery input/output V_{BAT}. Both fuses are fast-blow and rated for 3 A. In case the battery fuse fails, the battery pack still has its own internal protection circuit.

Over Voltage Protection

Additional over-voltage protection for the battery comes in the form of the battery voltage ADC measurement. When the measured voltage on the ADC is higher than the $V_{BAT(MAX,ADC)}$ during charging, the charger can be turned off via a microcontroller GPIO pin. There are also higher-voltage signals, that are scaled down to the logic level via a voltage divider so that they can be interfaced with the microcontroller pins. An example is the battery voltage ADC pin. These pins are in danger of overvoltage when the input rises beyond an upper threshold. 3.5 V varistors are connected between the ground and the logic-level signals to protect the microcontroller pins from overvoltage.

Under Voltage Protection

Discharging the battery below a certain threshold reduces its lifespan dramatically. To prevent the under-voltage of the battery, the battery voltage is monitored during the discharge cycle. Once the battery reaches $V_{BAT(MIN)}$, the microcontroller can pull down the Killswitch pin of the soft power switch controller, which leads to the whole ECU turning off. Unless the user charges the manipulation platform above the $V_{BAT(MIN)}$ threshold, he should not be able to turn it on. The working principle of the soft power switch is explained in 5.7.8.

Overheating Protection

The stepper drivers and the DC/DC buck converter controller have their own internal thermal shutdown protection. For additional protection, a temperature sensor is placed on the ECU. Its electrical schematic can be found in appendix 4. It is connected to the microcontroller via the I2C digital interface. The microcontroller would poll the data from the sensor periodically. Once the measured temperature shows an anomaly during charging, run time, or standby, the microcontroller can indicate this to the user, turn off the charger, or use the Killswitch pin of the soft power switch controller to cut the battery power from the ECU.

5.7.8 Manipulation Platform Power Switch

Switching the manipulation platform ON and OFF by a toggle switch that instantly cuts the power of the ECU by disconnecting the battery is not safe because of two things. First, when the motor is running and the user decides to switch off the manipulation platform by the toggle switch, the back EMF of the running motor could damage the ECU. Second, the ECU can be in the middle of an important data transfer from or to the data storage. Disconnecting the power could potentially corrupt the data from the data storage. To prevent this from happening, the design uses a tactile switch and a soft power switch controller, just like a PC or any other application that is sensitive to sudden power loss does.

Tactile ON/OFF Switch

The tactile ON/OFF switch features an LED ring, which can be changed to a red, green, or blue (RGB) color. Each LED color is connected to a 5 V voltage bus and an N-channel MOSFET, that is driven by a microcontroller pin. This allows simple color switching which is useful for signaling different states of the manipulation platform to the user. To interface the tactile switch and its LEDs with the ECU, a 6-pin PicoBlade connector is used.

Soft Power Switch Controller

The concept of a soft power switch is very simple. Whenever the platform is OFF, the user can momentarily press the tactile switch, which powers up the manipulation platform. The platform initializes itself and then enters the standby mode, where it is ready to perform the desired functionality. When the user wants to turn it off, he presses the tactile switch momentarily again, which gives a signal to the microcontroller to initiate the power down sequence. This sequence can have a lot of varying functionality, like stopping the motors and finishing the data storage transaction. Once the power down sequence is finished, the manipulation platform turns itself off.

The only issue is the fact, that in order to turn the device off, the microcontroller has to pick up the OFF indication from the button and execute the power down sequence. This may be impossible in case the microcontroller gets stuck due to a firmware bug and therefore the user would not be able to turn the platform off.

This can be resolved by allowing the user to hold down the tactile switch for a longer time, which forces a hard shutdown of the system's power, regardless of the state of the platform. This is once again often found in PCs and laptops.

To add all the above-mentioned functionality, a soft power switch controller is used. The soft power switch controller is an integrated circuit, that is powered by the battery and draws only a very small amount of leakage current in the range of μA. The battery is held back from powering the ECU by a P-channel MOSFET. The controller then drives the MOSFET ON or OFF exactly as explained above.

Additional circuitry is added for the case when the user wants to charge the manipulation platform. Forcing the user to turn the platform ON every time he wants to charge the device is inconvenient. So whenever the AC/DC adapter is plugged in by the user, the charger bypasses the soft power switch controller, drives the P-channel MOSFET to its ON state, and the ECU gets powered ON. Having the ECU always ON during charging also ensures that all protections mentioned in 5.7.7 are active.

5.7.9 Efficient Power Usage

With smaller manipulation platforms, the battery's capacity can be very limited. Therefore it is crucial to boost its run-time as much as possible by efficient design. One way to achieve that is to use high-efficiency components for power distribution. Another way to boost run-time is by allowing the firmware designer to turn off parts of the ECU that are not used at the time. Following is a typical example from the field of computer tomography.

The user uses the manipulation platform to precisely position his object of interest. Once positioned, he starts the scanning process which can take up to two hours. During this scanning process, most of the platform's functionality is not used and it only wastes the battery's energy.

Both options of efficient design are explored in the following chapters.

Power Buses

To power all the components on the ECU, there are a total of 4 power buses. The battery voltage level, 5 V, 3.3 V and 1.8 V. To efficiently convert the battery voltage to the 5 V and the 3.3 V voltage levels, two LTM8074 DC/DC buck converters are used. They are chosen mainly because of their package size, which measures only 4 mm x 4 mm.

Because the components that are powered by the 1.8 V bus draw very little current, using a linear dropout regulator (LDO) is sufficient. To keep the efficiency of the LDO high, the 3.3 V bus is connected to its input.

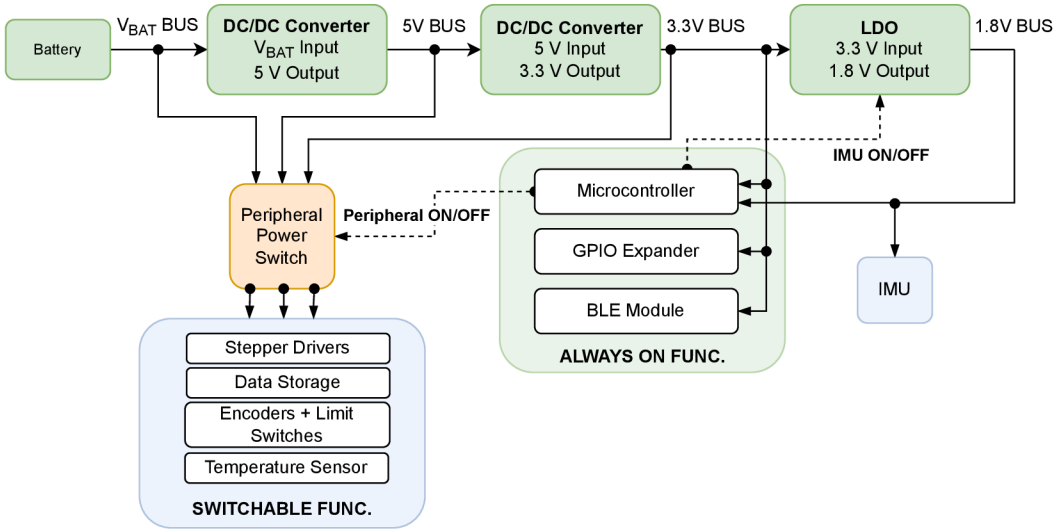

Figure 5.23: Power Distribution Diagram with Peripheral and IMU Switches

Peripheral Power Switches

Turning off a selection of circuits whose functionality is not required at the moment can be done by using the peripheral power switch. The peripheral power switch design consists of N-channel and P-channel MOSFETs, that are driven to their ON state or OFF state by a single microcontroller GPIO pin. The ECU's power distribution and switchable functionality are shown in the Figure 5.23.

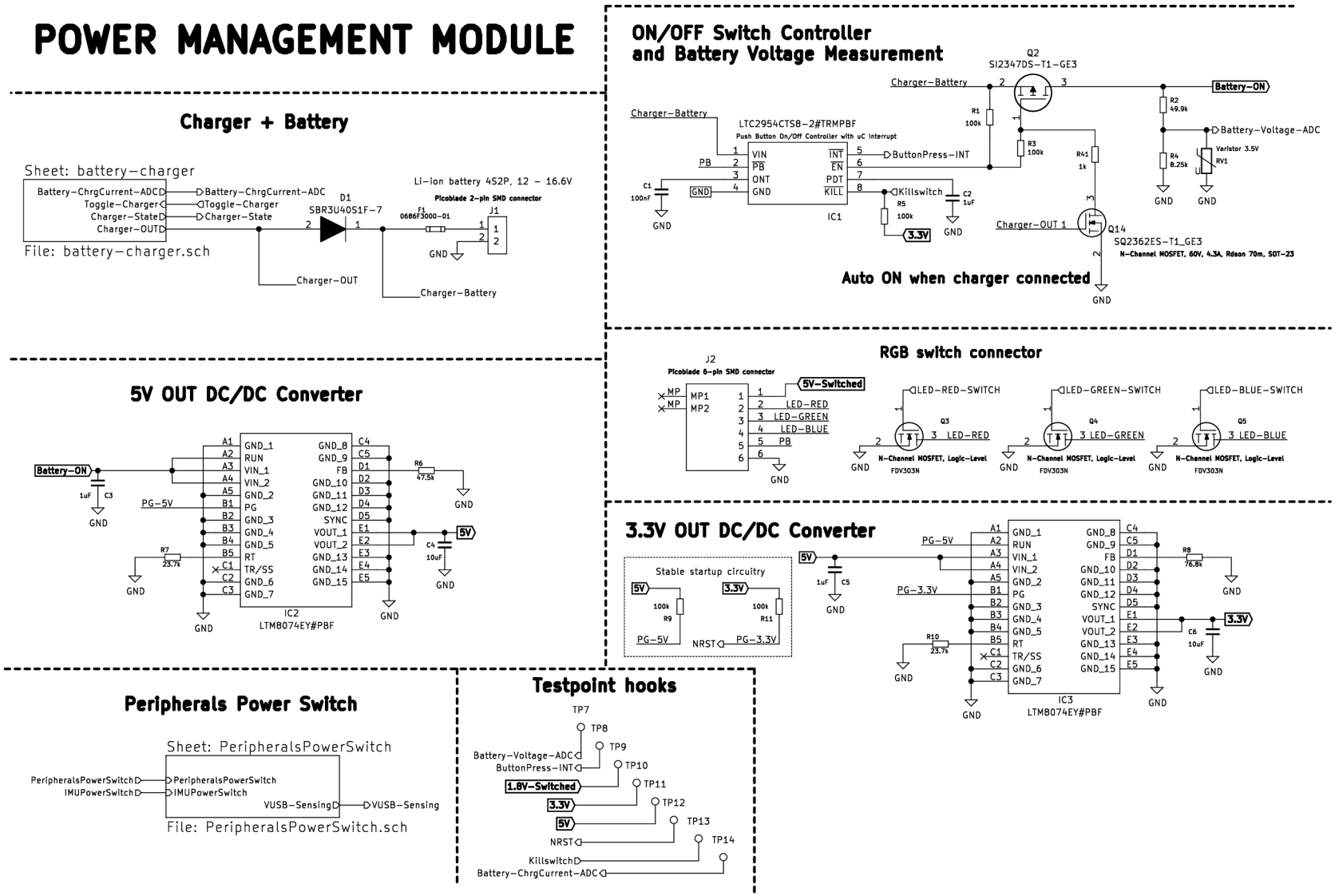

Figure 5.24: Power Management Module Electrical Schematic

5.8 Microcontroller

The microcontroller is the central point of the whole ECU, which holds all the functionality together. Picking the wrong one can lead to extended development times, which in turn lead to additional development costs. To pick the right microcontroller for the ECU, it is essential to first define what is expected from it.

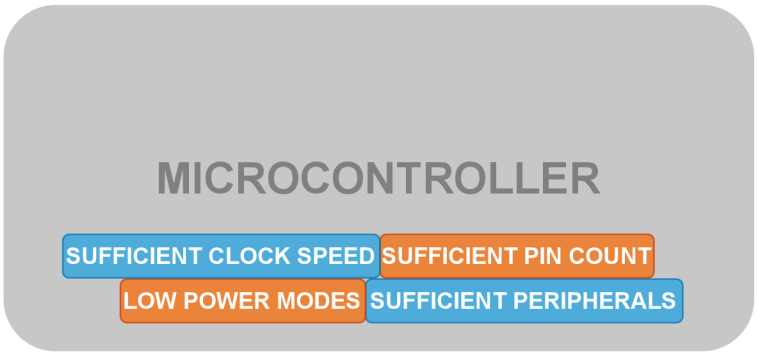

Figure 5.25: Microcontroller Design Requirements Block

The most obvious requirements come from all the chosen and designed ECU circuits in the previous sections. A summary of the required number of GPIO pins and additional functionalities per the ECU subsystem can be seen in the Table 5.6. The table reveals the following. A total of 51 GPIO pins is required. The required digital interfaces are 3xSPI (stepper drivers, encoders and GPIO expander use different types of SPI), 2x I2C (one of them 1.8 V compatible), 2x UART, 1x USB, and 1xSWD. The additional required peripheral functionality is 2x PWM generation outputs, 2x 32-bit timers, and 2x ADCs.

Table 5.6: Summary of ECU System Requirements for the Microcontroller

	No. of GPIO pins	**Additional func.**
2x Stepper Drivers	18	1xSPI, 2xPWM Output, 2x32 bit Timer
4x Limit Switches	4	NONE
2x Encoders	2	1xSPI
IMU	1	1xI2C (1.8V)
BLE Module	9	1xUART
FRAM Memory	3	1xSPI
Debug / Service	4	1xSWD, 1xUSB, 1xUART
Power Man. Mod.	9	2xADC, 1xI2C
GPIO Expander	1	1xSPI

Another set of parameters, such as the clock speed, flash memory size for the firmware, several interrupts (both internal and external), direct memory access (DMA), and addi-

tional timers come from the firmware design itself. It is very hard to predict these parameters before the firmware design is finished. Because of this, prototypes usually use the best, most expensive processor from the family of processors, which have the best parameters. Once the prototype is completed, tested, and verified, the required parameters are known and the processor's parameters can be scaled down to match the required parameters. The scaled-down processor is then used in the series production to save on the production cost.

Last but not least, the development time is also influenced by the tools the developer is given. Some microcontroller manufacturers offer additional support in terms of software, code libraries, and debugging tools, which can speed up the development process rapidly.

STM32L476 Microcontroller

The ECU is designed with STM32L476, which is an ultra-low-power microcontroller based on the ARM Cortex M4, operating at a frequency of up to 80 MHz [47].

Its main peripheral features are a Floating point unit (FPU), three fast 12-bit ADCs with multiple channels, two general-purpose 32-bit timers, two 16-bit PWM timers for dedicated motor control, and seven general-purpose 16-bit timers. It also features standard and advanced communication interfaces, such as three I2Cs, three SPIs, two UARTs, one Low-Power UART, one SWD, and one USB full-speed interface.

It is powered by 3.3 V and allows up to 14 GPIO pins or their alternate functions to work on an independent power source, which can be as low as 1.08 V. This feature is used for interfacing the microcontroller with the 1.8 V I2C that the IMU uses, which removes the need for logic level shifters.

Another great feature is the comprehensive set of power-saving modes, that allow the design of low-power applications.

Last but not least, the ST ecosystem of developer software, code libraries, and debugging tools is one of the best in the industry and truly reduces the development time of an application.

One of the drawbacks of this design is the microcontroller package choice. The chosen package has 144 pins. Even with all the GPIO pins, the digital interface pins, and additional functions pins, almost half of the pins are left unconnected. The package measures 20 mm x 20 mm which is a substantial amount of space, which does not truly conform to the miniaturization requirement.

However, choosing a package of this size is not a deliberate design choice. It is the only option due to the global component shortage[1] that is happening during the ECU design phase. To reduce the chances of this happening again in the future, a solution is proposed in the Subsection 5.8.1.

The microcontroller's electrical schematic is designed according to the manufacturer's recommendation in [47]. The schematic can be found in appendix 16.

5.8.1 GPIO Expander

To counter the ongoing global component shortage, which heavily affects the ST microcontroller supply chain, a GPIO expander is implemented onto the ECU.

The GPIO expander would be used for the times when a package with a high enough

[1] Global electronic component shortage happened in the year of 2021 and 2022 due to the global pandemic that happened in the year of 2020 and 2021.

pin count of the chosen ST microcontroller is not available.

The working principle of a GPIO expander is very simple. The GPIO expander has a set amount of pins, that can be used as GPIO pins. It uses a digital interface to communicate with the microcontroller. The microcontroller commands the GPIO expander to set its individual pins as inputs or outputs and is also able to read, set, and reset them via the commands.

The GPIO expander is obviously not needed for this ECU prototype since the chosen microcontroller package has more pins than is required. However, it is beneficial to develop the firmware with the GPIO expander in mind in case it is needed. The GPIO expander is therefore implemented and used on the ECU.

MAX7301ATL+ GPIO Expander

This GPIO expander features 28 GPIO pins, that can be individually configured to be a logic input or a logic output [48]. The expander uses SPI as its digital interface with the microcontroller. It also has a special interrupt pin interface, that can be programmed to indicate a change of state in a selected range of input pins. It has a very low standby current and it is offered in a small TQFN package.

For this ECU prototype, a selection of I/O signals is connected to the expander instead of connecting them to the microcontroller. This is done for the purpose of robust firmware development as mentioned in the Subsection 5.8.1. The designed electrical schematic can be found in appendix 11.

5.9 Printed Circuit Board Design

This section briefly goes through the PCB design challenges and design choices. The final PCB design schematic is shown in the Figure 5.27 and a detailed 3D Model with section labels can be found in the Figure 5.28.

The proper functioning of the ECU is highly dependent on a good PCB design. Designing a mixed-signal PCB of a very small size is a challenging process. The smaller the dimension of the PCB, the harder it is to keep the sensitive analog circuitry away from fast switching digital circuits and power converters, that induce noise in the analog signals.

The PCB design quality is heavily influenced by the PCB stack-up, component layout, grounding techniques, trace spacing, via placement, thermal management, and many others. The grounding techniques and component layout are the most important of all the above-mentioned parameters. Without proper return current paths, the board could face substantial electromagnetic interference (EMI) problems and would not pass the EMC testing.

5.9.1 PCB Stackup

Because of the space constraints of the ECU and the fact that it is a mixed-signal PCB, it is designed as a 6-layer board with components on both sides of the board. The board stack-up follows the design advice in [49] and can be seen in the Table 5.7. To reduce the EMI emissions, the ground planes are full with no cuts in them.

Table 5.7: PCB Stackup

Layer 1	– – – –	Signal
Layer 2	————	Ground
Layer 3	– – – –	Signal
Layer 4	– – – –	Power
Layer 5	————	Ground
Layer 6	– – – –	Signal

5.9.2 Component Layout

The first and most important step, that dictates the rest of the PCB design is the component layout. The 3D model of the PCB, which can be found in the Figure 5.28 clearly shows that the layout follows the recommendation from [49], which states that the digital section, the power section, and the analog section must have sufficient spacing between them to ensure good signal integrity.

Battery Charger Layout

Because the battery charger layout is the most critical one, it is discussed in more detail in this section. The charger consists of a fast switching power stage and a sensitive analog section. The fast switching power stage of the battery charger is kept to the bottom right

of the PCB (Figure 5.28). The sensitive analog section of the battery charger controller is above the controller, away from both the power section and other digital components. The Figure 5.26 shows this in more detail. It also shows the switching loop on the top side of the PCB, which consists of the input capacitor (Cin), the high-side switch (HSS), the low-side switch (LSS), and the current sense resistor (Rs). This loop is usually the highest source of EMI emissions. To reduce them, the switching loop is contained in as small an area as possible. The bottom side of the PCB shows the rest of the power stage's input and output capacitors and heatsink areas that are discussed in the subsection 5.9.3.

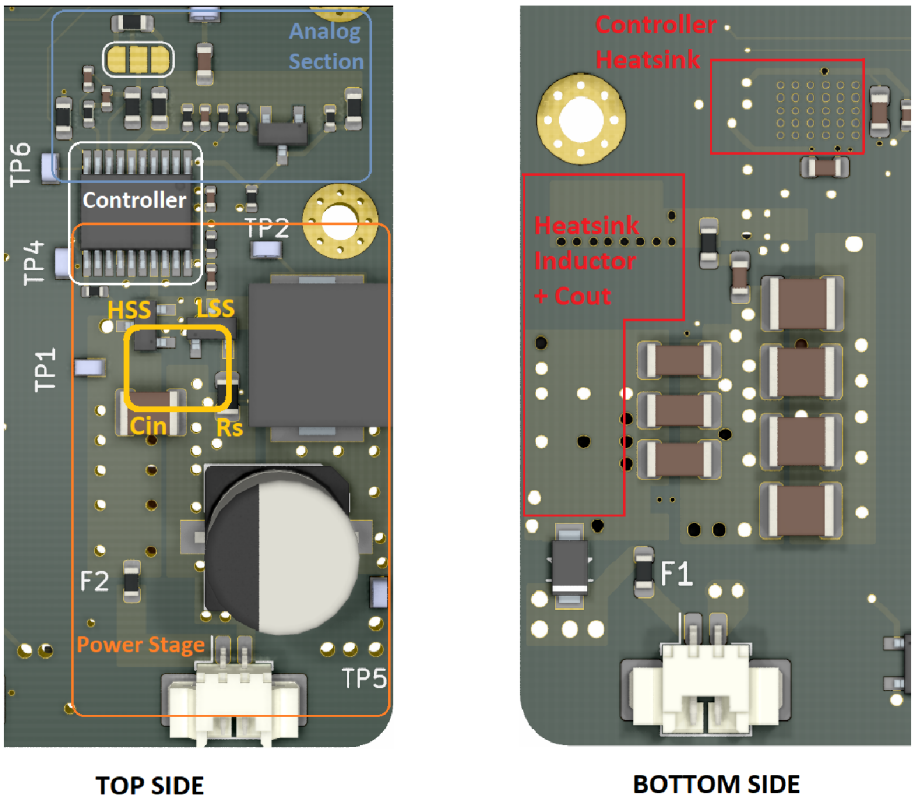

Figure 5.26: Battery Charger Layout, 3D Model Detail

5.9.3 Thermal Management

Three main power circuits generate most of the heat. Two of them are the stepper motor drivers and the third one is the battery charger's power stage.

Stepper Driver's Cooling System

Both stepper drivers have a thermal pad on the bottom side of their package, that is connected to the ground. There are two ground planes in the PCB, which help with the heat spread. In case the prototyping and testing Chapter 6 reveals insufficient cooling of the drivers, the stepper driver's ground pads are filled with thermal vias. Thermal vias lead most of the heat to the bottom side of the board, where a foam heatsink can be used to dissipate the heat into the manipulation platform's internal case. Reserved foam heatsink areas on the bottom side of the PCB are shown in red squares in the Figure 5.28.

Battery Charger's Cooling System

The battery charger's power stage is expected to heat up substantially, especially during the CC charging phase. The first step to cool down the power stage's components is to use thermal vias and copper pours in the internal layers to spread the heat into other layers of the board. Multiple thermal vias are deployed around the high side switch, the low side switch, and the inductor (Figure 5.26).

With all the heat being dissipated in the power stage, the controller will start to heat up as well. The controller has a thermal pad on the bottom side of its package that is connected to the ground. A grid of thermal vias is used here as well.

In case the prototyping and testing Chapter 6 reveals, that the cooling of the charger's individual components is insufficient, the Figure 5.26 shows the reserved foam heatsink areas. The heat would once again be dissipated into the manipulation platform's internal case.

5.9.4 Test Points

To smooth out the testing process of the ECU prototype, around 60 test points (TP) are used throughout the PCB. The top side of the PCB uses special test points that provide hook access to the oscilloscope probes. The bottom side of the PCB is designed with small round 1 mm test point pads. These pads are mainly used to test individual digital interfaces, such as the SPI and I2C, using a logic analyzer.

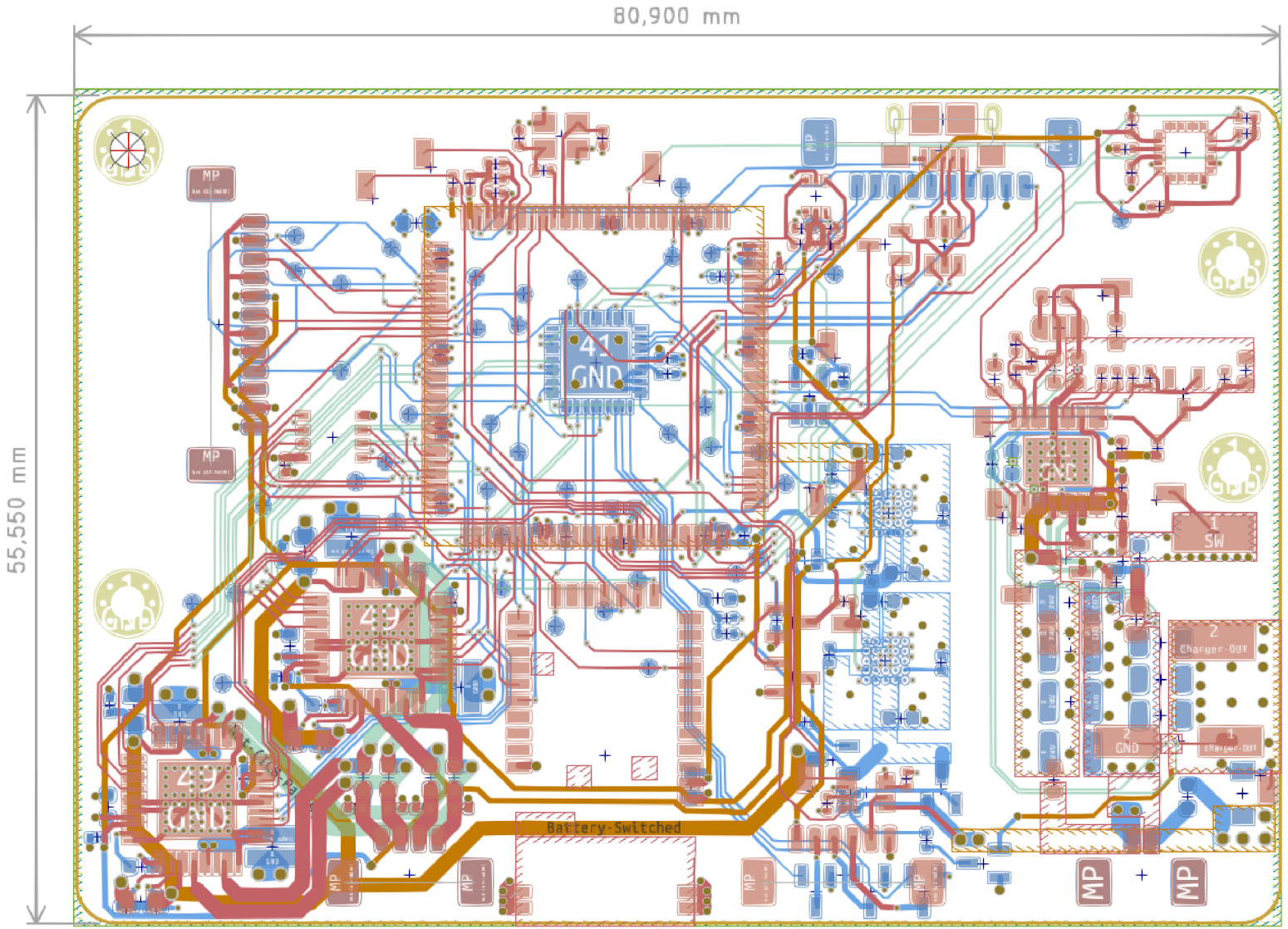

Figure 5.27: PCB Schematic, 6 Layers, Components on Both Sides. **Note:** Schematics of individual layers can be found in the appendixes 17 to 22

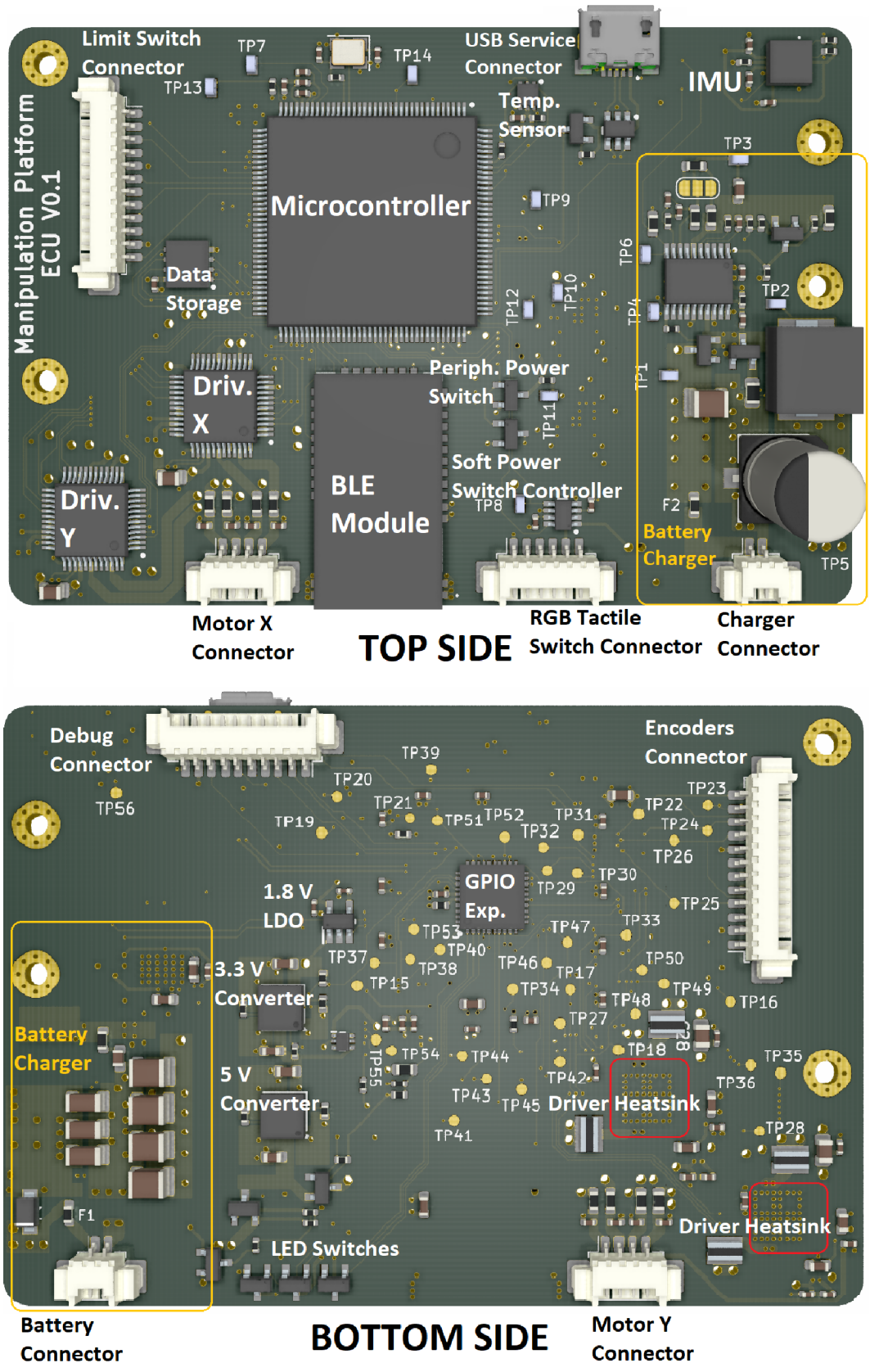

Figure 5.28: Labelled 3D Model of the ECU Printed Circuit Board.
Note: Includes USB and peripheral power switch corrections mentioned in the Section 6.7

6 Prototyping and Testing

This chapter ensures that all the building blocks of the ECU are correctly connected and designed so that the firmware developer is not held back by an oversight in the ECU design. The testing process consists of test cases that verify the designed functional blocks that stem from the concept diagram created in Chapter 4.

Some of the functionalities are tested by a digital multimeter and an oscilloscope, however, basic blocks of test firmware and software must be developed to test all of the functionalities of the ECU.

The test firmware is developed by using the STMCubeMX software, which allows the developer to create a functional pinout of the chosen microcontroller. All the required microcontroller peripherals, such as ADCs, digital interfaces, timers, clock sources, etc. are set up by using STMCubeMX's code generation tool. The generated initialization code is used as a baseline for all the testing that requires the microcontroller functionality. The STMCubeIDE software is then used for further development of the test firmware. The code for the ECU's test firmware is written in the C programming language.

The ECU is programmed by its debugger connector described in Subsection 5.6.2 and an ST-link-V2 programmer, which features the SWD interface.

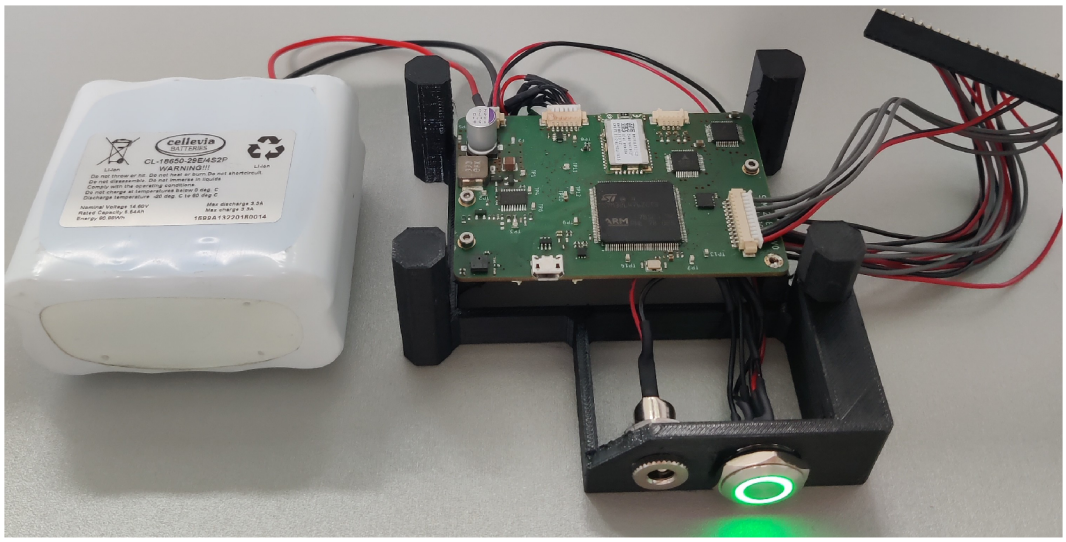

Figure 6.1: Manufactured ECU Prototype Mounted on a Test Stand

6.1 Prototype Manufacturing

With the electrical, PCB, and assembly schematics done, the ECU and limit switch boards are sent to the manufacturer. All schematics are designed in KiCad software. Due to the usage of very small SMD packages, such as BGA packages, the assembly of the ECU is done by an external company that specializes in the assembly of PCB prototypes. Limit switches SMD components are soldered manually by a soldering iron. All the required cabling and connector crimping is done manually as well.

The designed and manufactured ECU prototype measures 81 mm x 56 mm. For the purpose of testing, it is mounted on a specially designed 3D printed test stand, that allows easy access from both sides of the ECU. The setup can be seen in the Figure 6.1.

6.2 PMM Testing

The PMM testing process consists of multiple test cases that ensure the proper working of all the functionalities provided by the PMM. The individual functionalities that are being tested are shown in the testing diagram in the Figure 6.2.

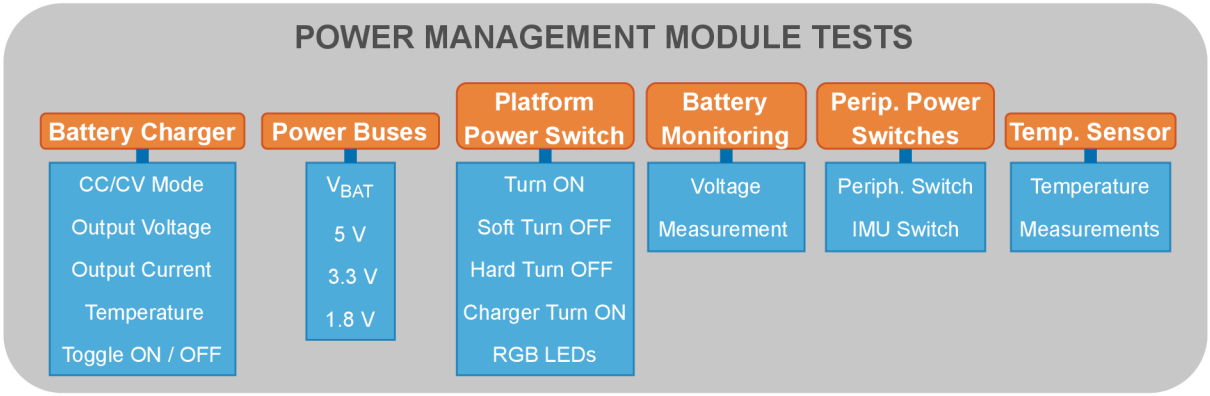

Figure 6.2: Power Management Module Test Diagram

Power Buses

Power buses are measured by both the oscilloscope and the digital multimeter. The Table 6.1 shows, that all measured buses are within tolerance. The battery voltage bus is also measured and it corresponds with the battery voltage level.

Table 6.1: Verification of Power Bus Voltage Levels

Designed	Measured
1.80 V	1.80 V
3.30 V	3.29 V
5 V	4.81 V

Battery Charger, Battery Monitoring, and Temperature Sensor

A library of basic functions is developed for the temperature sensor. The library consists of functions that allow the read/write of a specific register, using the I2C digital interface. The I2C interface is successfully tested by a logic analyzer. This library is provided for further firmware development for this ECU in [31]. The battery charging current and battery voltage is measured by the microcontroller's ADC.

First, the AC/DC adapter is plugged into the external battery charger connector which is a part of the 3D printed test stand. The charger, battery monitoring system, and temperature sensor are then successfully tested during a battery charging test, as can be seen in the Figure 6.4. The data logging is done by using the STMStudio software, which allows the logging of firmware variables via the SWD interface.

The waveform in the Figure 6.3 shows the switch node of the DC/DC converter very close to the end of the charging process. The measured switching frequency and the maximum output voltage of the DC/DC converter correspond to the designed values.

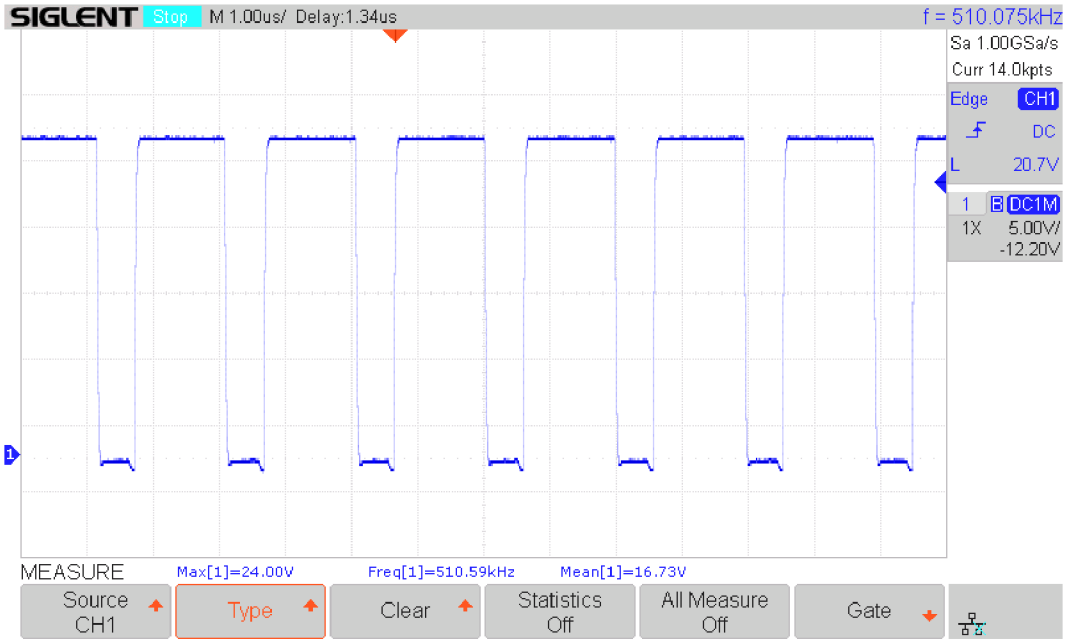

Figure 6.3: Switch Node of the DC/DC Buck Converter

Looking at the Figure 6.4, the battery's maximum RMS charging current is measured as 2.25 A and the battery's maximum charging voltage is measured as 16.53 V. Both values are within the tolerance of the design. The microcontroller is programmed to turn the charger off once the charging current drops to less than 5 % of the maximum charging current. This can be seen at the end of the charging test. The temperature sensor also works as expected. To verify the thermal design of the ECU's battery charger, individual components are measured by an infrared temperature meter during the charging process. Maximum temperatures are shown in the Table 6.2. All these components are rated for a junction temperature of 150 $°C$ and therefore have no issue with such temperatures. However, this is possibly the worst-case scenario, because the ECU is mounted to a plastic test stand, which has more thermal resistance than the metal case of a manipulation platform and no heatsinks are used.

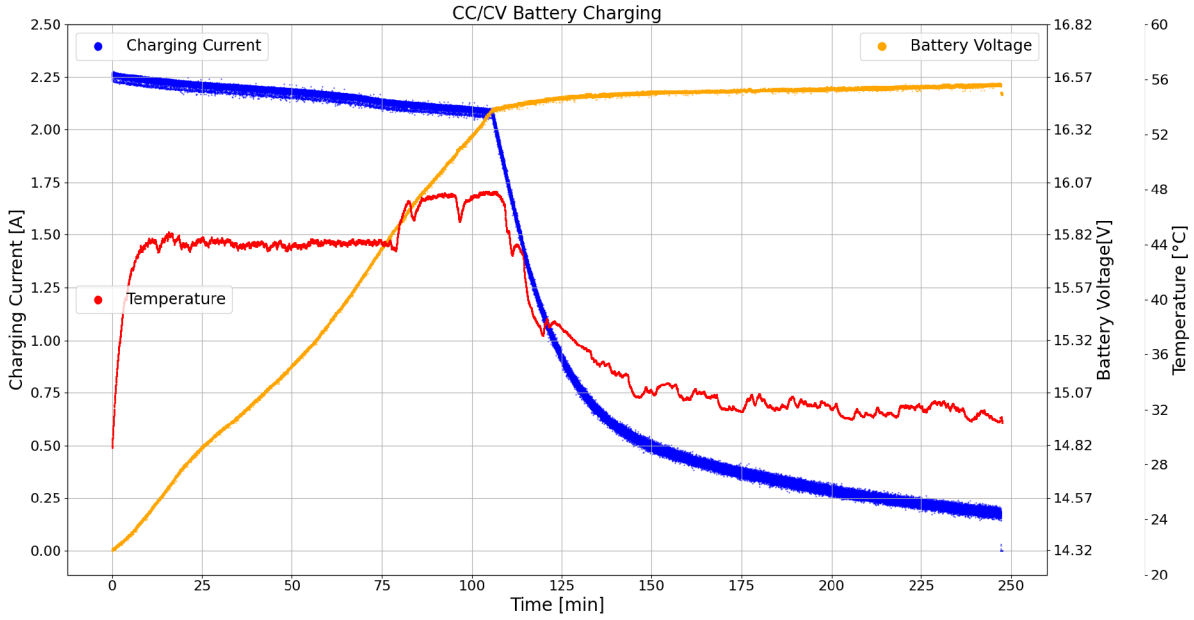

Figure 6.4: Battery Charging Test

Table 6.2: Maximum Temperature of Individual Components During Battery Charging

Component	**Maximum Temperature**
Power Stage Inductor	86.0 $°C$
High Side NMOS	80.8 $°C$
Low Side NMOS	85.0 $°C$
DC/DC Buck Controller	75.0 $°C$
Output Capacitor	72.0 $°C$

Manipulation Platform Power Switch and ECU Current Consumption

The power switch is a part of the 3D printed test stand, as can be seen in the Figure 6.1.

The design is successfully tested. Pressing the tactile switch for 1 s switches on the P-channel MOSFET, which in turn powers up the whole ECU.

While ON, the short press of the tactile switch is indicated to the microcontroller via an external interrupt pin. The debouncing of the tactile switch is automatically done inside the soft power switch controller. In the interrupt callback function, the microcontroller pulls the killswitch pin of the soft power switch controller low, which leads to the opening of the P-channel MOSFET and therefore to a soft turn OFF of the whole ECU.

The hard turn OFF is tested as well. Pressing the button down for more than 5 seconds while ON leads to the opening of the P-channel MOSFET and the whole ECU powers down without any intervention of the microcontroller.

Plugging in the AC/DC Adapter into the external battery charger connector successfully bypasses the soft power switch controller and turns the P-channel MOSFET ON, which powers the ECU.

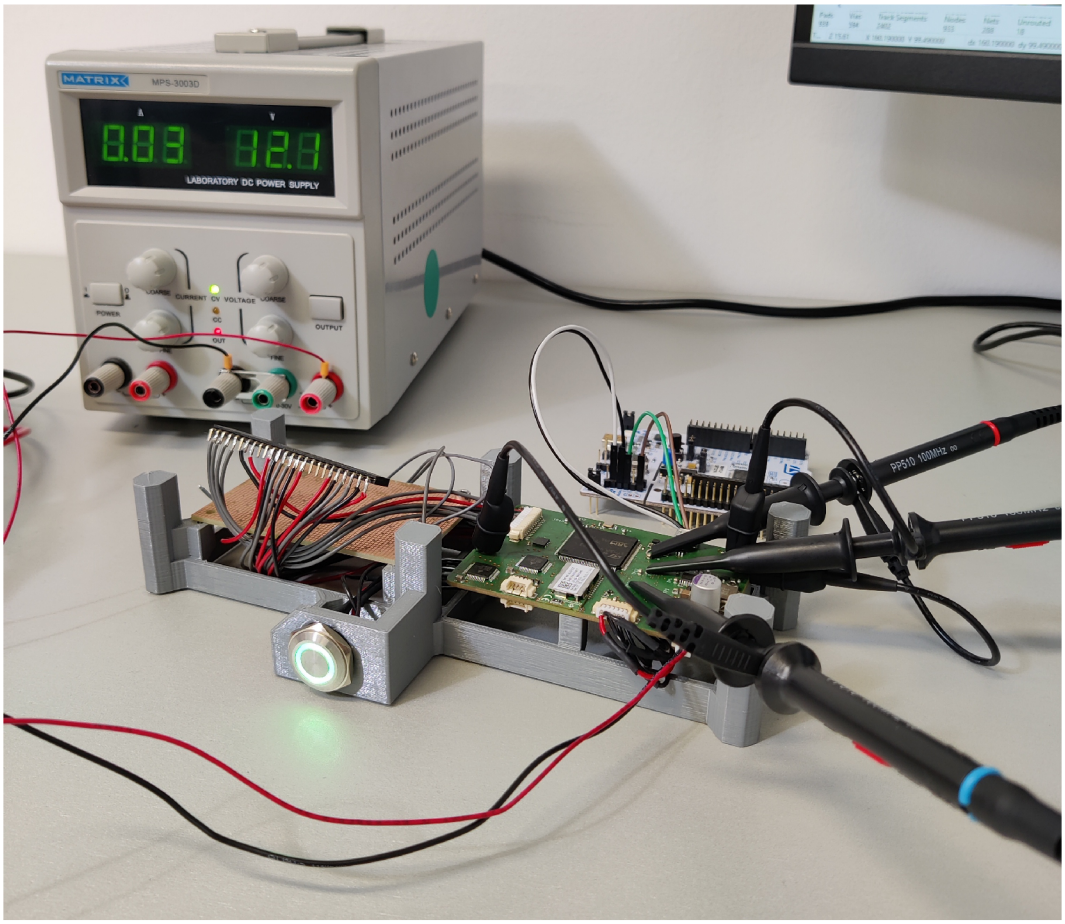

Figure 6.5: Illustrative photo of the ECU mounted on an alternative test stand, showing the usage of hook probe test points

The indication RGB LEDs of the power switch are controlled by the GPIO expander's pins. The GPIO expander communicates through the SPI interface. The SPI interface is successfully tested by a logic analyzer and a basic library of functions is developed. The functions are capable of configuring the GPIO expander's pin modes and pin states via the SPI interface in a convenient way. This library of functions is used for further firmware development in [31].

The current consumption of the ECU in standby mode is 23 mA to 30 mA, depending on the color of the LED. In the standby mode, the motors and encoders are not running but everything else on the ECU is turned ON, including the active BLE communication. With this current consumption, the battery of the manipulation platform would last for more than 7 days. However, to save as much of the battery's capacity for the positioning run-time of the manipulation platform, the current consumption can be more than halved in the future by smart firmware usage of peripheral power switches and the low power optimization of the microcontroller and the BLE module.

6.3 XY Motion Testing

The XY Motion functionalities that are being tested are shown in the Figure 6.6.

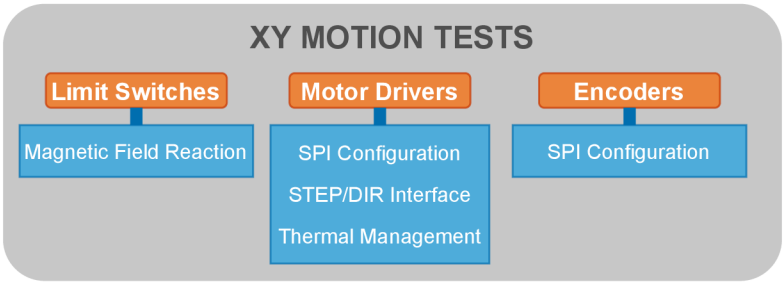

Figure 6.6: XY Motion Test Diagram

Motor Drivers

The motor drivers are tested by three test cases. The first one uses a logic analyzer soldered to the test points to ensure that the SPI is correctly connected and that the drivers can be configured via them. This test is successful.

For the second test, a code snippet borrowed from [31] is adapted to this test case, and the motors are spun in both directions via the STEP/DIR interface. This verifies that the drivers are operational and wired correctly.

In the third test, both motors are driven simultaneously to test the thermal management of the motor drivers. In this prototype, the motors are driven with very low current, which would not be sufficient to test the thermal management of the motor drivers. To test it properly a 0.4 A RMS current is chosen as a representative value. The motors are driven with the chosen current and after one minute, the temperature of both driver packages is measured by an infrared temperature meter. No heatsinks are used for this test. The measured temperatures are shown in the Table 6.3. Based on the results, the passive cooling of the package's thermal pad and thermal vias is shown to be sufficient for this test. However, for the maximum current rating of the motor driver (1.2 A RMS), foam heatsinks would have to be applied as specified in the 5.9.3.

Table 6.3: Thermal Management Test of Motor Driver X, Y

Motor Driver X	65.5 $°C$
Motor Driver Y	67.0 $°C$

Limit Switches

To verify the functionality of limit switches, all four limit switches are connected to the ECU. The signal pins of limit switches are connected to the microcontroller's GPIO input pins that have an internal pull-up resistor. The pin state is read while moving a small magnet back and forth the limit switch, simulating the motion of the motor carriage. The input pins effectively change their state from log. 1 to log. 0. every time the magnet is in close proximity to the limit switch. This corresponds with the expected behavior.

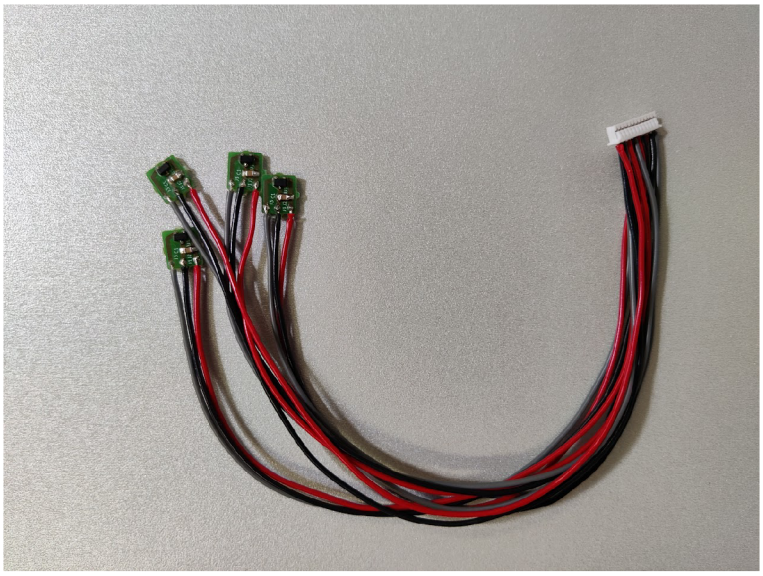

Figure 6.7: Limit Switches Cable Harness

Encoders

The encoders are connected by a single 12-pin connector and communicate via SPI. The SPI interface functionality is verified via a logic analyzer. The encoders are then successfully configured by using a code snippet provided by [31].

6.4 Wireless Control Testing

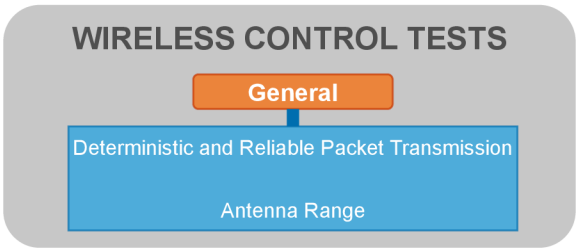

Figure 6.8: Wireless Control Test Diagram

The functionalities that are being tested are shown in the Figure 6.8. To test the capabilities of the designed wireless control solution, the BLE USB dongle is plugged into the PC and a BLE software application is developed on the PC side (Figure 6.9). A detailed description of the BLE protocol stack is beyond the scope of this thesis, however, the [51] and the Microsoft BLE C# documentation [50] are both great resources on this topic. The developed application can scan the nearby BLE devices, find the ECU's BLE module, and automatically connect to it. The core of this application is used for further software development in [31].

On the ECU side, a test firmware is created that puts the BLE module in the auto-pattern mode. The auto-pattern mode of the BM70 is briefly explained in the Subsection 5.4.1. The microcontroller talks to the BLE module via a UART interface.

To verify the determinism and reliability of wireless communication, the following test

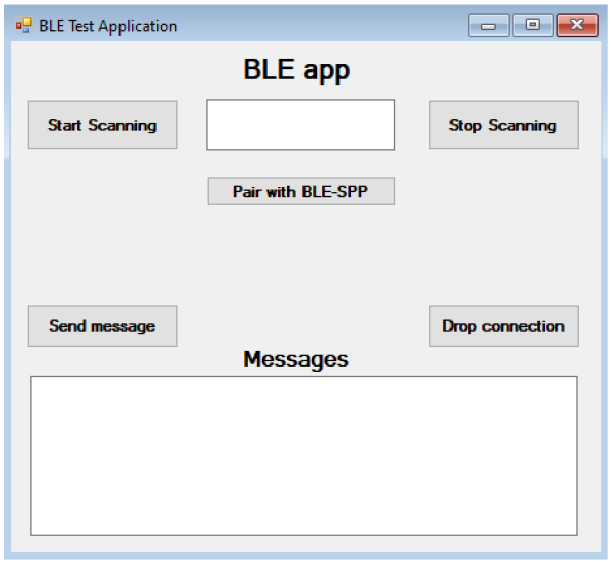

Figure 6.9: Windows BLE Test Application

case is created. Utilizing the developed PC application, command packets with 48 bytes of data are sent to the ECU each 100 ms. Every time the ECU receives the command packet, it replies with an echo packet of the same size. The packet length and communication timing emulate the communication protocol devised in [31]. Each command packet is numbered so that when it is received back by the PC, it can be recognized. Knowing when each packet is sent and received is useful for creating a graph of packet loss (reliability) and packet delay (determinism). Every echo packet that arrives to the PC with a delay of 100 ms or more is considered lost because a new command packet is already sent out by the PC application.

During the test, the ECU is surrounded by aluminum plates, that simulate the metal enclosure of the manipulation platform. There are no other obstacles between the ECU and the PC's BLE USB Dongle. A range of 2 m is chosen for this test. The resulting packet loss and packet delay of the test is shown in the Figure 6.10. As it can be seen, a total of 2823 command packets are transmitted by the PC application and a total of 2821 echo packets are received under the 100 ms limit by the PC application. 2 packets are above the limit and are therefore considered lost. The average echo packet delay is calculated as 49.8 ms.

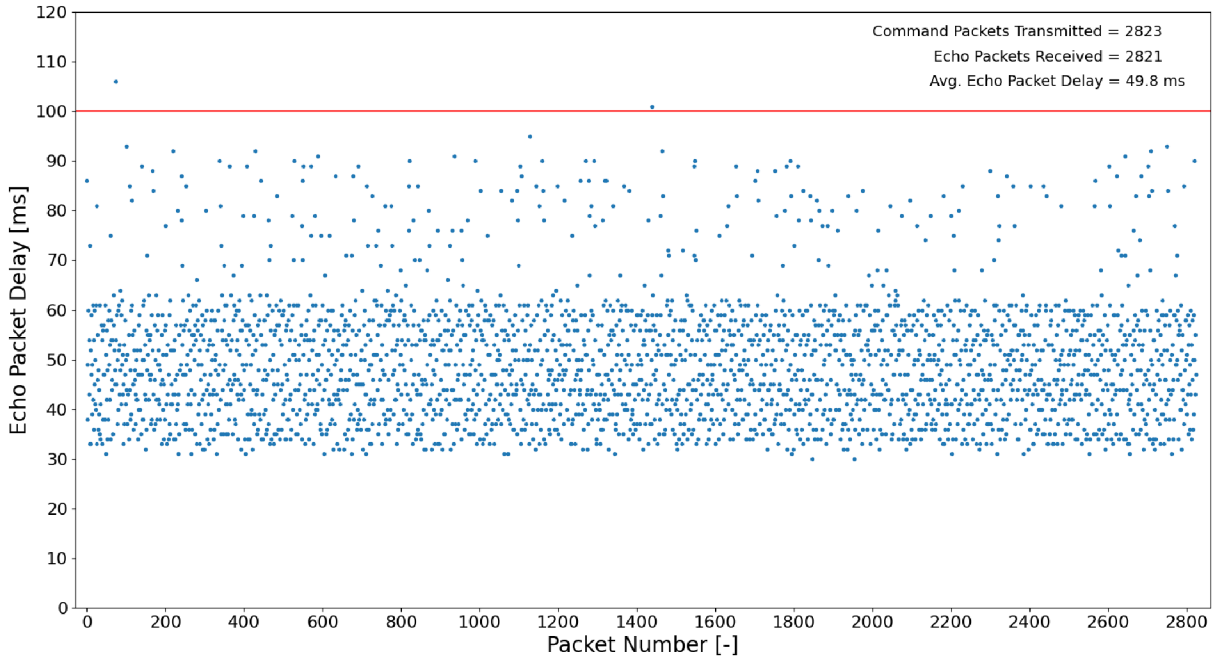

Figure 6.10: Packet Loss and Packet Delay Graph

This test proves that real-time, deterministic, and reliable wireless control is achieved. However, more optimization of the BLE module's parameters can be done via the extensive manual mode mentioned in 5.4.1. The above-mentioned test case is also tried for a range of 5 m. The results do not show any significant difference in packet delay or packet loss. Therefore, the antenna range of the BLE Module and USB BLE Dongle can be concluded as sufficient for this application.

6.5 Data Storage Testing

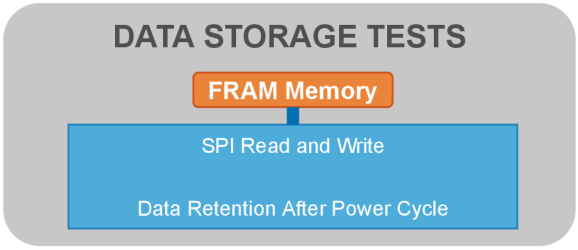

Figure 6.11: Data Storage Test Diagram

The functionalities that are being tested are shown in the Figure 6.11. A simple test firmware is created, that writes the word "FRAM" into the data storage memory via the high-speed SPI interface. The ECU is then turned OFF and ON again. The word "FRAM" that was written to the data storage is then read back and compared to the written value. This test case tests both the SPI interface and the data retention of the data storage unit.

A successful test can be seen in the Figure 6.12, where two logic analyzer scopes are shown. The first one shows the write transaction, where the word "FRAM" is written

into a specific address of the data storage as 4 bytes. The ECU is power cycled and the saved word is successfully read back from the data storage as shown in the second logic analyzer scope.

A small library of functions is then created for the FRAM memory. The library provides convenient writing and reading functionality. The library is also used for further firmware development in [31].

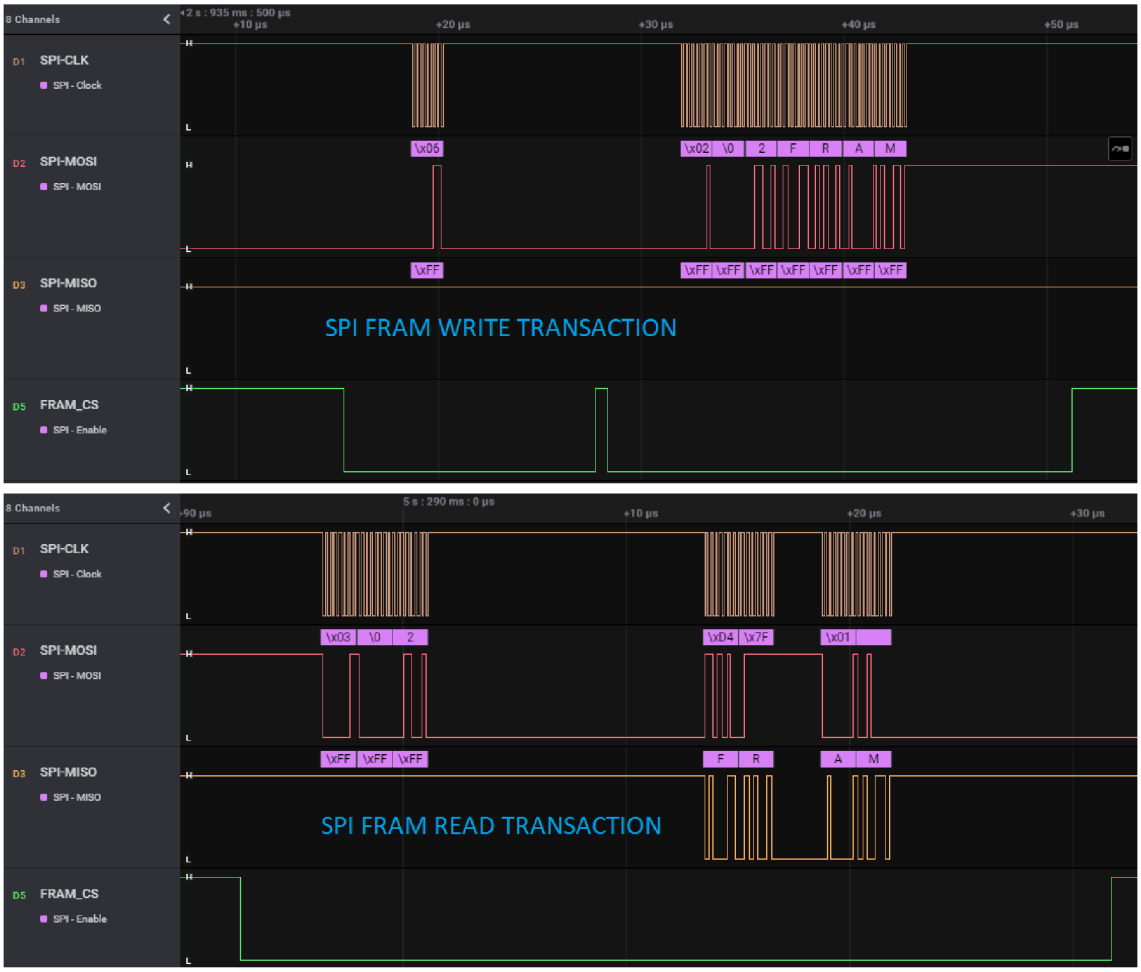

Figure 6.12: Data Storage - Write and Read Transaction

6.6 IMU Testing

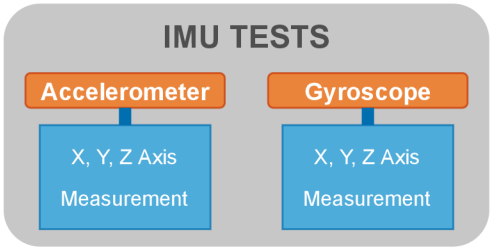

Figure 6.13: IMU Test Diagram

The functionalities that are being tested are shown in the Figure 6.13. The IMU uses a digital 1.8 V I2C interface to communicate with the microcontroller. The interface is successfully tested via a logic analyzer. The IMU's gyroscope, accelerometer, sampling rate, and internal digital low pass filter are then configured.

A small library of functions is developed and successfully tested. The library allows for convenient configuration and measurement of each accelerometer and gyroscope axis. The visualization of the measurements is shown in the control software developed by M. Remiš [31].

6.7 Prototype Evaluation

The ECU prototype is evaluated and its individual functions are successfully tested by the defined test cases in the sections above.

Two issues were found during the testing procedure. The USB service connector and peripheral power switches are not operational due to a design oversight. Neither of these features is critical to the functionality of the ECU. The design of both features has been corrected and a new ECU is already being manufactured. No other problems were found during the testing process.

The ECU prototype satisfies the design requirements that were defined by the concept diagram in Figure 4.1. Further development and testing are done in the thesis of Matuš Remiš [31], where a fully functioning firmware for the ECU prototype is developed, together with a PC control software. He also implements the ECU into the test stand for the manipulation platform control system prototype as shown in the Figure 6.14.

Figure 6.14: Test stand of the manipulation platform control system prototype [31]

7 Conclusion

The thesis is one part of a team project that deals with the development of a control system for a wireless, battery-powered manipulation platform application. The system consists of an electronic control unit, firmware, and PC control software. The development of the control system firmware and software is done in Matuš Remiš's thesis [31].

The main goal of this thesis is to conceptualize, design, prototype, and test the ECU for the proposed manipulation platform control system.

The chapter 3 of this thesis deals with the research of used technical solutions for standard manipulation platform control systems. It introduces the basic terminology and the system diagram of a manipulation platform control system. More attention is then given to the standard control hardware and control software that is used in the industry. Because the proposed system is battery-powered and wirelessly controlled in real-time, the research also describes battery technology options, battery charging, and the challenges of real-time wireless control. A small section is also given to the Bluetooth Low Energy technology. Bluetooth Low Energy technology is used for the wireless control of the platform because of its low current consumption, adaptability, and its relatively deterministic and reliable protocol.

In the chapter 4, a set of control system functional requirements is defined. The set of requirements of the system is based on the standard functionalities of similar industrial platforms, such as the one described in 3.1.3. Based on this set of functional requirements, the ECU concept design diagram (Figure 4.1) is created. The concept diagram systematically divides the ECU into functional blocks. It specifies the following functional blocks: XY motion, wireless control, power management module, IMU, data storage, debug and service interface, and a microcontroller. It also specifies general requirements, such as miniaturization of the ECU and thermal management. It does not specify the motor type or battery type and therefore it can be used as a baseline for designing with various motor or battery technologies.

The ECU is systematically designed in the chapter 5. The design sections are logically divided by closely following the functional blocks defined in the concept diagram. The first major part (Section 5.2) of the design is the XY motion functional block. There, two stepper motor drivers, limit switches boards and encoder connectors are designed. The stepper drivers are robust enough to be used with various stepper motors. The soft limit switch design utilizes a hall sensor, which reacts to the presence of a magnetic field. Limit switches are also designed as compact as possible so that they can be fitted even inside very small manipulation platforms.

The second major part (Section 3.4) implements a BLE module on the ECU and chooses a BLE USB dongle for the PC. This allows the wireless control of the manipulation platform. The BLE module was chosen based on its small dimensions, low energy consumption, and decent antenna range. One of its major features is the auto-pattern mode, which heavily simplifies the implementation from the firmware point of view. The

second major feature is the manual mode, which allows the developer to optimize the BLE protocol stack parameters. This feature will be very useful in the future endeavors of this project.

The third major part (Section 5.7) deals with the design of the power management module. The designed module handles power buses, battery monitoring, battery charging, a soft power switch for turning the manipulation platform safely ON and OFF, and a peripheral power switch, which allows for efficient power control. Indication LEDs and safety measures, such as over-current, over-voltage, under-voltage, and overheating protection are included in the power management module design.

Li-ion battery technology is chosen for the prototype due to its compact size and high capacity. The battery voltage is monitored by the microcontroller ADC whenever the system is turned ON. This is done for safety purposes and rough capacity estimation. The battery charger is designed with adaptability and robustness in mind and can be adapted to different battery voltages just by replacing a few component values. This kind of adaptability makes the ECU very simple to implement in manipulation platforms with different battery voltage requirements. The overall charging process is designed to be as straightforward for the user as is charging a laptop.

The ECU design chapter also deals with the implementation of minor functionalities, that are defined in the concept diagram. The first minor functionality is the data storage unit, which is used for storing default control parameters of the manipulation platform. In the future of the project, the data storage will also be used for storing additional information such as manufacturing date and ID, long-term battery data, and user-defined macros. The second minor functionality is the design of a low power inertial measurement unit (IMU), which features a gyroscope for tracking the rotation of the manipulation platform's XY coordinate system. This unique feature helps the operator of the platform with positioning tasks inside a computer tomography system. Third and last minor feature is the USB interface service connector and debug connector. The debug connector utilizes the Serial Wire Debug interface, which brings additional functionalities when paired with the STMStudio software. The USB service connector allows direct connection to the PC, which may be necessary for future servicing or tuning of the control system. The USB service connector will be mainly used for the user firmware update functionality, which will be developed in the future of the project.

All the above-mentioned functionalities are tied together and controlled by a single ARM Cortex M4 microcontroller. Since the chosen microcontroller family has been hit by the global component shortage of 2022, the section 5.8 tries to keep the ECU design robust by implementing a widely available GPIO expander as a stand-in for situations, when the microcontroller package has an insufficient number of GPIO pins.

Overall, the ECU design uses efficient and low-power components. Furthermore, the section 5.9.3 deals with the design of the thermal management system of power electronics. Due to the dimensional limitations of a standard manipulation platform interior, there is also a substantial emphasis on the miniaturization of the ECU. Thanks to the efficient PCB layout shown in the Section 5.9, small SMD packages, 6-layer PCB stack-up, and utilization of both sides of the PCB, the final dimensions of the ECU are only 56 mm x 81 mm. This allows the whole control system to be used even in very compact manipulation platforms.

Eventually, the designed ECU prototype is manufactured and assembled and each individual functionality is tested in the chapter 6. Except for minor issues with the

USB interface and peripheral power switches, the ECU design satisfies all the functional requirements of the concept diagram. The outcome of this thesis is therefore a fully functioning ECU prototype, whose functionality is further verified by Matuš Remiš in his thesis [31].

The final outcome of the team project is a functional prototype of a wireless control system, which can be implemented into preexisting manipulation platforms. This project can be followed up by both a bachelor's or a master's thesis. The thesis can focus on further expansion of ECU functionalities via an expansion board, development of advanced firmware and software functionalities, or possibly a creation of a mechanical design of a manipulation platform with this control system in mind.

Bibliography

[1] Motion Basics Terminology & Standards. Newport [online]. Newport Corporation [cit. 2022-05-16]. Available at: https://www.newport.com/n/motion-basics-terminology-and-standards

[2] Accuracy vs. Repeatability. In: Newport [online]. Newport Corporation, ©2022 [cit. 2022-05-16]. Available at: https://www.newport.com/medias/sys_master/images/images/h0a/hc4/8797577740318/Accuracy-figure-S-600w.gif

[3] M-971 Motorized OEM XY Stage. In: Physik Instrumente [online]. Auburn: Physik Instrumente [cit. 2022-05-16]. Available at: https://static.pi-usa.us/fileadmin/_processed_/b/e/csm_M-971.01_bff2625888.jpg

[4] Digital Motion Controllers for Precision, Dynamics, and Operating Convenience. Physik Instrumente [online]. Auburn: Physik Instrumente [cit. 2022-05-16]. Available at: https://www.pi-usa.us/en/expertise/technology/controllers-software/precision-motion-control/

[5] Motion Control Software / Tools. Physik Instrumente [online]. Auburn: Physik Instrumente [cit. 2022-05-16]. Available at: https://www.pi-usa.us/en/products/controllers-drivers-motion-control-software/motion-control-software/

[6] 2,048 Microstep Resolution Achieved with New Cost-Effective Compact Stepper Motor Controller. Physik Instrumente [online]. Auburn: Physik Instrumente [cit. 2022-05-16]. Available at: https://www.pi-usa.us/en/news-events/news/news-detailpage/2048-microstep-resolution-achieved-with-new-cost-effective-compact-stepper-motor-controller/

[7] C-663.12 Mercury Step Stepper Motor Controller, 1 Axis. Physik Instrumente [online]. Auburn: Physik Instrumente [cit. 2022-05-16]. Available at: https://www.pi-usa.us/en/products/precision-motion-controllers-and-drivers-for-positioning-systems/c-66312-mercury-step-stepper-motor-controller-900553/

[8] XY Stages - Precision Motorized Planar XY Positioning Stages. Physik Instrumente [online]. Auburn: Physik Instrumente [cit. 2022-05-16]. Available at: https://www.pi-usa.us/en/products/precision-motorized-linear-stages/integrated-xy-precision-motorized-stages-planar-xy-stages/

[9] M-971 Motorized OEM XY Stage. Physik Instrumente [online]. Auburn: Physik Instrumente [cit. 2022-05-16]. Available at: https://www.pi-usa.us/en/products/precision-motorized-linear-stages/integrated-xy-precision-motorized-stages-planar-xy-stages/m-971-motorized-oem-xy-stage-412418464/

[10] C-663.12 Mercury Step Stepper Motor Controller, 1 Axis. In: Physik Instrumente [online]. Auburn: Physik Instrumente [cit. 2022-05-16]. Available at: https://static.pi-usa.us/fileadmin/_processed_/b/5/csm_C-x63.12_ff844dde9e.jpg

[11] C-663.12 Mercury Step Stepper Motor Controller, 1 Axis, Back Panel. In: Physik Instrumente [online]. Auburn: Physik Instrumente [cit. 2022-05-16]. Available at: https://static.pi-usa.us/fileadmin/_processed_/3/3/csm_PI_C-863_12_rear_325b404694.jpg

[12] BUCHMANN, Isidor. BU-104c: The Octagon Battery - What makes a Battery a Battery. Battery University [online]. 2021 [cit. 2022-05-16]. Available at: https://batteryuniversity.com/article/bu-104c-the-octagon-battery-what-makes-a-battery-a-battery

[13] BUCHMANN, Isidor. BU-214: Summary Table of Lead-based Batteries. Battery University [online]. 2021 [cit. 2022-05-16]. Available at: https://batteryuniversity.com/article/bu-214-summary-table-of-lead-based-batteries

[14] BUCHMANN, Isidor. BU-301a: Types of Battery Cells. Battery University [online]. 2021 [cit. 2022-05-16]. Available at: https://batteryuniversity.com/article/bu-301a-types-of-battery-cells

[15] BUCHMANN, Isidor. BU-216: Summary Table of Lithium-based Batteries. Battery University [online]. 2021 [cit. 2022-05-16]. Available at: https://batteryuniversity.com/article/bu-216-summary-table-of-lithium-based-batteries

[16] BUCHMANN, Isidor. BU-204: How do Lithium Batteries Work?. Battery University [online]. 2022 [cit. 2022-05-16]. Available at: https://batteryuniversity.com/article/bu-204-how-do-lithium-batteries-work

[17] BUCHMANN, Isidor. BU-215: Summary Table of Nickel-based Batteries. Battery University [online]. 2021 [cit. 2022-05-16]. Available at: https://batteryuniversity.com/article/bu-215-summary-table-of-nickel-based-batteries

[18] BUCHMANN, Isidor. BU-203: Nickel-based Batteries. Battery University [online]. 2021 [cit. 2022-05-16]. Available at: https://batteryuniversity.com/article/bu-203-nickel-based-batteries

[19] BUCHMANN, Isidor. BU-409: Charging Lithium-ion. Battery University [online]. 2021 [cit. 2022-05-16]. Available at: https://batteryuniversity.com/article/bu-409-charging-lithium-ion

[20] BUCHMANN, Isidor. BU-304: Why are Protection Circuits Needed?. Battery University [online]. 2021 [cit. 2022-05-16]. Available at: https://batteryuniversity.com/article/bu-304-why-are-protection-circuits-needed

[21] BUCHMANN, Isidor. BU-908: Battery Management System (BMS). Battery University [online]. 2021 [cit. 2022-05-16]. Available at: https://batteryuniversity.com/article/bu-908-battery-management-system-bms

[22] BUCHMANN, Isidor. Charge states of lithium ion. In: Battery University [online]. 2021 [cit. 2022-05-16]. Available at: https://batteryuniversity.com/img/content/ion1.jpg

[23] Atanasov, Svetoslav. (2013). An Overview of Wireless Communication Technologies Used in Wireless Sensor Networks. International Scientific Conference eRA-8. ISSN-1791-1133. 11-18. Available at: https://www.researchgate.net/publication/262565993_An_Overview_of_Wireless_Communication_Technologies_Used_in_Wireless_Sensor_Networks

[24] Bluetooth Technology Overview. Bluetooth [online]. [cit. 2022-05-18]. Available at: https://www.bluetooth.com/learn-about-bluetooth/tech-overview/

[25] BM70 BLE Module. In: Microchip [online]. [cit. 2022-05-18]. Available at: https://www.microchip.com/content/dam/mchp/mrt-dam/products/poe/150904-WPD-PHOTO-IS1870-plus-BM70-9x6.jpg

[26] RONDÓN, Raúl, Mikael GIDLUND a Krister LANDERNÄS. Evaluating Bluetooth Low Energy Suitability for Time-Critical Industrial IoT Applications. International Journal of Wireless Information Networks [online]. 2017, 24(3), 278-290 [cit. 2022-05-17]. ISSN 1068-9605. Available at: doi:10.1007/s10776-017-0357-0

[27] Bluetooth Core Specification Version 5.0 Feature Enhancements [online]. 2017, 12 [cit. 2022-05-17]. Available at: https://www.bluetooth.com/wp-content/uploads/2019/03/Bluetooth_5-FINAL.pdf

[28] MARCEL, Jason. How Bluetooth Technology Uses Adaptive Frequency Hopping to Overcome Packet Interference. Bluetooth [online]. 2020 [cit. 2022-05-17]. Available at: https://www.bluetooth.com/blog/how-bluetooth-technology-uses-adaptive-frequency-hopping-to-overcome-packet-interference/

[29] LAKKAS, George. MOSFET power losses and how they affect power-supply efficiency [online]. Texas Instruments Incorporated, 2016 [cit. 2022-05-17]. Available at: https://www.ti.com/lit/an/slyt664/slyt664.pdf?ts=1651655059930&ref_url=https%253A%252F%252Fwww.google.com%252F

[30] Stepper Motor Parameters. In: Na 3D [online]. [cit. 2022-05-18]. Available at: https://www.na3d.cz/resize/e:ec99f/1200/1200/files/0-56.jpg

[31] REMIŠ, Matúš. Design of control system for manipulating platform [online]. Brno, 2022 [cit. 2022-05-18]. Available at: https://www.vutbr.cz/studenti/zav-prace/detail/139926. Master's Thesis. Vysoké učení technické v Brně, Fakulta strojního inženýrství, Institute of Solid Mechanics, Mechatronics and Biomechanics. Supervisor Zdeněk Hadaš.

[32] TMC2130-TA. In: Trinamic [online]. [cit. 2022-05-18]. Available at: https://www.trinamic.com/fileadmin/assets/Products/ICs_Images/TMC2130-TA.jpg

[33] TMC2130-LA. In: Trinamic [online]. [cit. 2022-05-18]. Available at: https://www.trinamic.com/fileadmin/assets/Products/ICs_Images/TMC2130-LA.jpg

[34] TMC 2130 Stepper Driver IC Datasheet [online]. 2014, (Version V1.09) [cit. 2022-05-18]. Available at: https://www.trinamic.com/fileadmin/assets/Products/ICs_Documents/TMC2130_datasheet.pdf

[35] Piccoblade 4 Pin Connector. In: Farnell [online]. [cit. 2022-05-18]. Available at: https://cz.farnell.com/molex/53261-1371/connector-header-13pos-1row-1/dp/3103089?st=53261-1371

[36] Micropower Omnipolar Digital Hall-effect Sensor ICs, SL353 [online]. [cit. 2022-05-18]. Availaible at: https://www.farnell.com/datasheets/2012449.pdf

[37] OrbisTM True Absolute Rotary encoder [online]. [cit. 2022-05-18]. Availaible at: https://www.rls.si/eng/fileuploader/download/download/?d=1&file=custom%2Fupload%2FBRD01_09_EN_data_sheet.pdf

[38] 7-Axis, High Performance Integrated 6-Axis Inertial and Barometric Pressure Sensor, ICM-20789 [online]. [cit. 2022-05-18]. Availaible at: https://3cfeqx1hf82y3xcoull08ihx-wpengine.netdna-ssl.com/wp-content/uploads/2017/10/DS-000169-ICM-20789-TYP-v1.4.pdf

[39] High Performance 6-Axis MEMS Motion Sensor and Pressure Sensor Combo, ICM-20789. In: Ivensense TDK [online]. [cit. 2022-05-18]. Availaible at: https://invensense.tdk.com/products/motion-tracking/7-axis/icm-20789/

[40] Bluetooth® Low Energy (BLE) Module, BM70 [online]. [cit. 2022-05-18]. Availaible at: https://ww1.microchip.com/downloads/en/DeviceDoc/Bluetooth-Low-Energy-BLE-Module-DS60001372K.pdf

[41] USB-BT400. In: Asus [online]. [cit. 2022-05-18]. Availaible at: https://www.asus.com/cz/Networking-IoT-Servers/Adapters/All-series/USBBT400/

[42] 64-Kbit (8K × 8) Serial (SPI) F-RAM, FM25CL64B [online]. Infineon [cit. 2022-05-18]. Availaible at: https://www.infineon.com/dgdl/Infineon-FM25CL64B_64-Kbit_(8_K_8)_Serial_(SPI)_F-RAM-DataSheet-v11_00-EN.pdf?fileId=8ac78c8c7d0d8da4017d0ebdfcd83119

[43] Rechargeable Li-ion battery pack, CL-18650-29E4S2P [online]. [cit. 2022-05-18]. Availaible at: https://www.tme.eu/Document/46bd8bff964efc6cc503d9a81e37c5c5/CL-18650-29E4S2P.pdf

[44] STEP MOTOR BASICS. Geckodrive [online]. [cit. 2022-05-18]. Availaible at: https://www.geckodrive.com/support/step-motor-basics.html

[45] Wide Input Range Synchronous Buck Controller with Analog Current Monitor, LM5117 [online]. Texas Instruments [cit. 2022-05-18]. Availaible at: https://www.ti.com/lit/ds/symlink/lm5117.pdf

[46] Automotive N-Channel 60 V (D-S) 175 °C MOSFET, SQ2362ES [online]. Vishay [cit. 2022-05-18]. Availaible at: https://www.vishay.com/docs/62913/sq2362es.pdf

[47] Ultra-low-power Arm® Cortex®-M4 32-bit MCU+FPU, STM32L476xx [online]. ST [cit. 2022-05-18]. Availaible at: `https://www.st.com/resource/en/datasheet/stm32l476je.pdf`

[48] 4-Wire-Interfaced, 2.5V to 5.5V, 20-Port and 28-Port I/O Expander, MAX7301 [online]. Maxim Integrated [cit. 2022-05-18]. Availaible at: `https://datasheets.maximintegrated.com/en/ds/MAX7301.pdf`

[49] How to Achieve Proper Grounding - Rick Hartley - Expert Live Training. Altium [online]. 2019 [cit. 2022-05-18]. Availaible at: https://resources.altium.com/p/emea-how-to-achieve-proper-grounding-rick-hartley-expert-live-training-6

[50] Bluetooth Low Energy - UWP Applications. Microsoft [online]. [cit. 2022-05-20]. Available at: https://docs.microsoft.com/en-us/windows/uwp/devices-sensors/bluetooth-low-energy-overview

[51] AFANEH, Mohammad. Intro to Bluetooth Low Energy [online]. V1.1. Novel-Bits, 2018 [cit. 2022-05-20]. Available at: https://www.novelbits.io/introduction-to-bluetooth-low-energy-book/

Appendix

The thesis contains following appendixes:

ECU electrical and PCB schematics.pdf

1. Manipulation Platform ECU - High Level
2. Peripherals - High Level
3. Encoders Connector
4. Temperature Sensor
5. FRAM Memory
6. Stepper Drivers
7. Trinamic Driver X
8. Trinamic Driver Y
9. HALL Limit Switches Connector
10. Bluetooth Module
11. GPIO Expander
12. Inertional Measurement Unit (IMU)
13. Power Management Module
14. CC/CV Battery Charger
15. Peripherals Power Switch
16. Microcontroller, Debug and USB Connector
17. Layer 1 - Signal
18. Layer 2 - Ground Plane
19. Layer 3 - Signal
20. Layer 4 - Power
21. Layer 5 - Ground Plane

22. Layer 6 - Signal

23. Limit Switch

24. Limit Switch Layer 1